The network interplay of interferon and toll-like receptor signaling pathways in the anti-Candida immune response

Ranieri Coelho Salgado (ranierics@usp.br)
University of São Paulo https://orcid.org/0000-0002-9660-9747

Dennyson Leandro M. Fonseca
Universidade Federal do Para https://orcid.org/0000-0003-2567-5808

Alexandre H. C. Marques
Dept. of Rheumatology and Clinical Immunology, University of Lübeck

Sarah Maria da Silva Napoleao
Institute of Biomedical Sciences, University of São Paulo

Tábata Takahashi França
University of São Paulo

Karen Tiemi Akashi
University of São Paulo

Caroline Aliane de Souza Prado
University of São Paulo

Gabriela Crispim Baiocchi
Institute of Biomedical Sciences, University of São Paulo

Desirée Rodrigues Plaça
Institute of Biomedical Sciences, University of São Paulo

Gabriel Jansen-Marques
University of São Paulo

Igor Salerno Filgueiras
Institute of Biomedical Sciences, University of São Paulo

Roberta De Vito
Princeton University

Paula Paccielli Freire
Institute of Biomedical Sciences, University of São Paulo https://orcid.org/0000-0003-0649-8279

Gustavo Cabral de Miranda
University of Sao Paulo

Niels Olsen Saraiva Camara
University of Sao Paulo

Vera Lúcia Garcia Calich

Institute of Biomedical Sciences-USP
Hans D. Ochs
University of Washington
Lena F. Schimke
Dept. of Rheumatology and Clinical Immunology, University of Lübeck
Igor Jurisica
University of Toronto
Antonio Condino-Neto
Institute of Biomedical Sciences, University of São Paulo
Otavio Cabral-Marques (otavio.cmarques@gmail.com)
University of São Paulo

Research Article

Keywords: Candida spp., Interferon signaling, Toll-like Receptors (TLR)

Posted Date: April 30th, 2021

DOI: https://doi.org/10.21203/rs.3.rs-279551/v2

The network interplay of interferon and toll-like receptor signaling pathways in the anti-Candida immune response

Ranieri Coelho Salgado[a], Dennyson Leandro M. Fonseca[b], Alexandre H. C. Marques[b], Sarah Maria da Silva Napoleao[a], Tábata Takahashi França[a], Karen Tiemi Akashi[b], Caroline Aliane de Souza Prado[b], Gabriela Crispim Baiocchi[a], Desirée Rodrigues Plaça[b], Gabriel Jansen-Marques[c], Igor Salerno Filgueiras[a], Roberta De Vito[d], Paula Paccielli Freire[a], Gustavo Cabral de Miranda[a], Niels Olsen Saraiva Camara[a], Vera Lúcia Garcia Calich[a], Hans D. Ochs[e], Lena F. Schimke[a], Igor Jurisica[f,g] Antonio Condino-Neto[a], Otavio Cabral-Marques[a,b,h]

[a]Department of Immunology, Institute of Biomedical Sciences, University of São Paulo, São Paulo, SP, Brazil.

[b]Department of Clinical and Toxicological Analyses, School of Pharmaceutical Sciences, University of São Paulo, São Paulo, SP, Brazil.

[c]Information Systems, School of Arts, Sciences and Humanities, University of Sao Paulo, São Paulo, SP, Brazil.

[d]Department of Biostatistics and the Data Science Initiative at Brown University, Providence, RI, USA.

[e]Department of Pediatrics, University of Washington School of Medicine, and Seattle Children's Research Institute, Seattle, WA, USA.

[f]Osteoarthritis Research Program, Division of Orthopedic Surgery, Schroeder Arthritis Institute, UHN; Data Science Discovery Centre, Krembil Research Institute, UHN; Departments of Medical Biophysics and Computer Science, University of Toronto, Toronto, Canada.

[g]Institute of Neuroimmunology, Slovak Academy of Sciences, Bratislava, Slovakia.

[h]Network of Immunity in Infection, Malignancy, and Autoimmunity (NIIMA), Universal Scientific Education and Research Network (USERN), São Paulo, SP, Brazil.

Correspondence to:

Ranieri Coelho Salgado
Department of Immunology
Institute of Biomedical Sciences - University of São Paulo
Lineu Prestes Avenue,1730, São Paulo, Brazil
Email: ranierics@usp.br
Phone: +55 11 30917435

Otavio Cabral-Marques, MSc, PhD
Department of Immunology
Institute of Biomedical Sciences - University of São Paulo
Lineu Prestes Avenue,1730, São Paulo, Brazil
Email: otavio.cmarques@usp.br
Phone: +55 11 974642022

ABSTRACT

Fungal infections represent a major global health problem that affects over a billion people and kills more than 1.5 million individuals annually. Here we employed an integrative approach to unravel the landscape of the human immune responses to *Candida spp.* (*C. albicans* and *C. auris*) by performing a meta-analysis of microarray, bulk, and single-cell RNA-sequencing (RNASeq) of blood transcriptome data. We identified that *C. albicans* activates a network interplay of signaling molecules commonly involved in both toll-like receptor (TLR) and interferon (IFN) signaling cascades. These molecules form a highly interconnected interferome network, which contains an immune overlap with the anti-viral responses. scRNAseq data confirmed that genes commonly identified by the three transcriptomic methods present a consistent upregulation pattern across innate immune and adaptive cells (CD4+, CD8+, and CD19+ lymphocytes). Thus, our results shed new lights on the molecular basis of immune response to *Candida spp*.

INTRODUCTION

Fungal infections, including the emergence of new fungal pathogens highly resistant to antifungal drugs, represent a major global health issue[1–5]. Fungal infections affect over a billion people worldwide and kill more than 1.5 million individuals annually. This mortality rate is similar to that of tuberculosis and 3-fold higher than that of malaria[6,7]. Invasive candidiasis (IC) is the most common fungal disease, affecting approximately 250,000 people annually and causing more than 50,000 deaths[8,9]. The increasing number of patients with human immunodeficiency virus (HIV) infection, malignancies, inborn errors of immunity (IEI), autoimmune diseases (receiving immunosuppressive treatment), and hematopoietic stem cell or organ transplant recipients contributes to this high frequency of individuals susceptible to life-threatening fungal pathogens[10,11]. The severity of fungal infections in healthy subjects ranges from asymptomatic or mild mucocutaneous manifestations to life-threatening systemic infections. These data reinforce the critical role of interactions between the microbial and host immune system in the outcome of infection[7,12], which needs to be further investigated to find new therapies to reduce morbidity and mortality caused by Candida infections[13,14].

Linear and mechanistic approaches have elegantly demonstrated that the anti-fungal immune response involves the appropriate recognition of pathogen-associated molecular patterns (PAMPs) by different pattern recognition receptors (PRRs) expressed on the cell membrane such as C-type lectin receptors (CLRs: dectin-1, dectin-2, and CD209), scavenger receptors (CD36), and toll-like receptors (TLRs: e.g., TLR2 and 4). Intracellular PRRs including RIG-I-like receptors (RLRs: melanoma differentiation-associated protein 5 or MDA5), TLRs (e.g., TLR3 and TLR9), and NOD-like receptors (NLRs: nucleotide-binding

oligomerization domain-containing protein or NOD1/2, NOD-, LRR- and pyrin domain-containing 3 or NLRP3) are also relevant and expressed by antigen-presenting cells and phagocytes, which bind to well-known ligands[15–17]. Activation of PRRs induces several signaling events such as the canonical Nuclear factor (NF)-κB pathway[18] that trigger effector anti-fungal mechanisms such as phagocytosis, production of reactive oxygen species (ROS)[19], degranulation, and neutrophil extracellular traps (NETs)[20,21]. Simultaneously, PRRs promote the production of key inflammatory cytokines such as tumor necrosis factor (TNF)-α, Interleukin (IL)-1β, IL-6, IL-17, type I Interferons (IFNs [IFN-α/β]), and the IL-12/IFN-γ axis[17,22–24], which shape and instruct immune cells[25].

However, the landscape of anti-fungal molecules in a holistic and integrative way remains to be provided. To reach this goal, we performed a meta-analysis of blood transcriptome data of microarray, bulk, and single-cell RNA-sequencing (scRNAseq) to unravel the landscape of the human immune responses to *Candida spp.* (*C. albicans* and *C. auris*). This integrative approach revealed a previous unnoted network interplay of type 1 interferon and toll-like receptor signaling in the anti-candida immune response.

RESULTS

C. albicans activates signaling molecules commonly involved in both toll-like receptor and interferon signaling cascades.

We surveyed published RNAseq datasets and found a total of 8 datasets related to the human immune response to *Candida spp*., being 5 of microarray, 2 bulk RNAseq, and one scRNAseq (further details in Methods section). We explored the scRNAseq by performing over representation analysis (ORA) of differentially expressed genes (DEGs) from innate immune (monocytes, natural killer, and plasmacytoid dendritic cells) and adaptive cells (CD4+, CD8+, and CD19+ lymphocytes), which were assigned to clusters as previously described (**Fig. 1a**). TCD4+ cells were most prevalent in the peripheral blood mononuclear cells (PBMCs). We found similar distribution pattern when assigning these cell types to clusters in resting and after *C. albicans* activation (**Fig. 1b-c**). A total of 6722 DEGs (**Suppl. Table 1**) were present in these clusters when comparing *C. albicans*-activated to resting cells. Enriched pathways associated with the immune response to *C. albicans* are shown in **Fig. 1d** while all enriched categories are present in **Suppl. Table 2**. Among them are 72 and 99 DEGs belonging to TLR and IFN (both type I and type II) signaling cascades, suggesting an interplay previously noted only in response to lipopolysaccharide (LPS)[26] . Across these DEGs there were 7 in common between both pathways. We also searched in literature and found more 55 DEGs involved in both TLR and IFN signaling cascades (**Suppl. Table 3**); totaling, thus 62 associated DEGs, six of them illustrated in **Fig. 1e-f.**

Modular gene co-expression analysis reveals an interplay of TLR- and IFN-associated genes

We next performed modular gene co-expression analysis[27], to better understand the interplay between TLR and IFN signaling cascades. For this analysis, we used the microarray dataset from Smeekens et al. (GSE42606)[28], the unique public dataset available containing more than 15 samples per group (30 resting and 24 *C. albicans*-activated samples), which is required to obtain biologically meaningful modular networks[29]. Modular gene co-expression analysis using CEMiTool[30] identified thirteen enriched co-expression modules from the total expressed genes by PBMCs (which contain lymphocyte subpopulations, monocytes, and dendritic cells). Among these modules, 12 were significantly enriched (9 downregulated and 3 upregulated) in response to *C. albicans* infection (**Fig. 2a**). Of note, modules M1 and M2 indicate gene co-expression and upregulation of IFN and interleukin signaling with TLR cascades (**Fig. 2b-e**).

Based on the results obtained by the modular co-expression analysis, we dissected the significantly enriched pathways from differentially expressed genes (DEGs) induced by *C. albicans*[28]. In agreement with the topological results obtained using CEMiTool, ORA of DEGs using the ClusterProfiler tool[31] pinpointed different clusters related to the activation of the TLR and IFN signaling cascades (**Suppl. Fig 1a-b**). IFN signaling was the most enriched pathway modulated by *C. albicans*. The relationship between the 30 most enriched pathways and their associated genes is shown in a network view (**Suppl. Fig 1c**) while the entire list of all enriched pathways is summarized in **Suppl. Table 4**. *C. albicans* activation significantly enriched several TLR signaling events such as TLR4, TLR3, TLR7/8, and TLR9 as well as MyD88/TIR-domain-containing adapter-inducing interferon-β (TRIF)/TIR Domain Containing Adaptor Protein (TIRAP) cascades, and TRAF6-mediated NF-κB activation. ORA also indicated that *C. albicans* activates chemokine (G protein-coupled receptors [GPCR]

ligand binding) and cytokine signaling pathways (IL-10, IL-3 and IL4), IFN-α/β signaling, Interferon-stimulated gene 15 (ISG15) antiviral mechanism, TNF Receptor Associated Factor 3 (TRAF3)-dependent IRF activation, DExD/H-Box Helicase 58 (DDX58)/Interferon Induced with Helicase C Domain 1 (IFIH1)-mediated induction of IFN-α/β, and regulation of type I and II IFN among the IFN signaling events (**Suppl. Fig 1a and c; Suppl. Table 4**).

C. albicans infection activates common TLR- and IFN-associated genes in peripheral blood leukocytes

We further investigated which DEGs and signaling pathways are consistently activated by *C. albicans* in peripheral blood leukocytes such as PBMCs (datasets GSE42606 and GSE154911) and peripheral white blood cells (WBCs, datasets GSE65088 and GSE114180) throughout all publicly available datasets. WBCs contain PBMCs (lymphocytes 20-45% and monocytes 2-10%) and granulocytes (neutrophils: 50-70%; basophils: 0-1%; and eosinophils: 1-5%)[32]. A meta-analysis of WBCs and PBMCs gene expression datasets using P-value combination method revealed among the meta-significant genes 44 commonly activated DEGs (40 upregulated and 4 downregulated) (**Fig 3a, Suppl. Table 5**). According to the cell population, these DEGs form well-defined hierarchical clusters, i.e., PBMCs datasets present a closer expression pattern among them as well as the WBCs datasets, when we compare both regulation and significance (**Fig 3b**). Enrichment analyses using EnrichR of these 44 genes revealed 87 significantly affected pathways (**Suppl. Table 6**), including TLR and IFN-α/β signaling pathways (**Fig. 3c**). Furthermore, these 44 DEGs also enrich other related interleukin signaling pathways such as JAK-STAT, IL-12, IL-17, IL-23, TNF, and chemokines (GPCR ligand binding) and PRRs, including RIG-I like receptor and NOD

signaling. Multi-study Factor Analysis of eligible[33] datasets (WBCs: GSE65088 and PBMCs: GSE42606; those with minimal number of samples required for this analyses) identified two common latent factors with high loadings, while specific latent factors showed low loadings across these studies. Thus, strengthening the biological relevance of these 44 common genes (**Fig. 3d, Suppl. Table 7**).

C. albicans activates common TLR and IFN signaling pathways across different layers of immunity

Subsequently, we added monocyte-derived dendritic cells (moDCs) datasets (GSE77969, E-MTAB-135, E-MTAB-751) into our integrative analysis. moDCs are known to be essential players of anti-fungal immunity, bridging the immune system's innate and adaptive arms. We searched for genes commonly regulated by *C. albicans* in transcriptomes of WBCs, PBMCs, and moDCs, in resting or *C. albicans* activation conditions. Intersection analyses performed according to cell population identified 123, 223, and 57 common DEGs among WBCs, PBMCs, and moDCs datasets, respectively (**Fig. 4a-c**). However, only 2 common DEGs were present across all seven datasets (**Fig. 4d**), which by themselves do not significantly enrich signaling pathways. We then asked if DEGs from each dataset enrich common signaling biological processes among all studies. Gene Ontology (GO) analysis using ClusterProfiler analysis revealed 173 common biological processes (**Suppl. Table 8**). We found several molecules/pathways essential for the anti-fungal immune response[34]. Among them, there is a cluster of IFN-γ, and NF-kB signaling, and a previously described overlap with the immune response to virus (IFN-α/β)[24] (**Fig. 4e**). Additional ORA of DEGs involved in this cluster found significant enrichment of signaling cascades of single TLRs (TLR2, TLR3, TLR4,

TLR5, TLR9, TLR9, and TLR10), TLR heterodimers (TLR1/TLR2, TLR2/TLR6, TLR7/8), and TLR adapter molecules (MyD88/TIRAP, TRAF6, TRIF) as well as several interleukin signaling pathways such as IL-1, IL-4/IL-13, IL-6, IL-10, IL-17, and IFN-α/β (**Fig. 4f)**. We found 1096 DEGs (**Suppl. Table 10**) affecting common biological processes among WBCs, PBMCs and moDCs. **Fig. 4g** shows the interactome obtained from some of these 1096 DEGs and enriched signaling cascades (**Suppl. Table 11**), thus highlighting the association of TLR- and IFN-signaling cascades, which were consistently enriched during our analyses. These 1096 DEGs also enrich other PRR and Interleukin signaling pathways such as CLRs (dectin-1), NLRs (NOD1/2), pro- (IL-1, IL6, IL-17, IL-12), anti-inflammatory (IL-10), and T helper 2 (IL-4 and IL-13) cytokines. This immunological balance between a pro-and anti-inflammatory event is crucial for the proper control of fungal infections while maintaining immune homeostasis[35,36].

C. albicans infection increases the correlation between TLR- and IFN-associated genes

After verifying TLR and type I and II IFN signaling cascades' consistency, we assessed the degree of association between these two variables during the immune response to *C. albicans*. Due to minimum sample size requirement[37], we selected TLR and IFN-associated genes present in the PBMCs transcriptome data from Smeekens et al. (GSE42606)[28]. This dataset contains 45 and 14 TLR- and IFN-associated DEGs modulated by *C. albicans* when compared to the resting group. *C. albicans* infection increased mainly positive correlations between TLR- and IFN-associated DEGs (**Fig. 5a-b**). We performed Canonical Correlation Analysis (CCA) to further assess the association's strength between TLR and IFN DEGs. CCA is a generic parametric model used to quantify relationships between two groups of

interrelated and interdependent variables[38]. This approach unveiled a pair of canonical variates (x-CV1 and y-CV1) highlighting the strong association between most of TLR - and IFN -associated DEGs in both resting and *C. albicans*-infected PBMCs (**Fig. 5c**), although, they are able to stratify these conditions (**Fig. 5d-e**).

The multidrug-resistant *C. auris* also induces the interplay between TLR and IFN signaling pathways

We asked if only *C. albicans* induces the association between TLR- and IFN-associated genes or also the multidrug-resistant *C. auris*[39,40]. We used the unique publicly available dataset analyzing the immune response to *C. auris* and *C. albicans* (GSE154911). Similar to *C. albicans* activation, ORA of DEGs induced by *C. auris* included TLR and IFN signaling cascades among the 30 most enriched pathways (**Fig. 6a-b**). *C. albicans* and *C. auris* similarly modulated DEGs' levels involved in TLR signaling, including NF-κB1, NF-κB2, JUN, and DUSP4, as well as IFN signaling such as IRFs, GBPs, SOCS1, ISG20, TRIM, and IFIT3 (**Fig. 6c**). When we compared the DEGs induced by *C. auris* with those enriching common pathways among all datasets (1096 DEGs, **Suppl. Table 10**) assessing the immune response to *C. albicans,* we identified 237 common DEGs (**Fig. 6d**). ORA of these common DEGs indicates that the interplay between TLR and IFN signaling cascades is a consistent immunologic feature in response to these two Candida species (**Fig. 6e**).

Inborn errors of immunity (IEI) corroborate the interplay between TLR and IFN signaling cascades

Finally, we aimed to evaluate the potential clinical and translational relevance of the TLR- and IFN-associated genes and molecular pathways consistently modulated by Candida. Therefore, we searched for IEI associated genes that are known to increase human susceptibility to fungal infections. So far, mutations in 100 genes have been associated with IEI that cause increased susceptibility to candidiasis and often other clinical manifestations. We compared them with the 1096 genes (**Suppl. Table 10**, i.e., those enriching the common biological processes activated by Candida (**Fig. 4e**). These 1096 genes encode molecules present in different cellular compartments such as extracellular regions, organelles, and nuclei and those forming macromolecular complexes. Together, they form a highly interconnected physical protein-protein interaction network (**Fig. 7a**), which contains several hubs[41] (**Fig. 7b**), here defined as those having more than or equal to 200 interaction partners. Of note, 34 genes associated with IEI are also present across the studies. Meanwhile, although 66 genes associated with IEI are not identified in the datasets, these genes are highly connected with the other DEGs in this network. Furthermore, the 1096 DEGs mostly contain Type I and II IFN- associated genes, being 868 in total (**Fig. 7c, Suppl. Table 12**).

The 34 IEI associated genes present in this network underly 7 groups of IEI including congenital defects of phagocytes, defects of intrinsic and innate immunity, predominantly antibody deficiencies, and diseases of immune dysregulation, as defined by the International Union of Immunological Societies Expert Committee(IUIS)[42] (**Suppl. Fig. 2a**). Notably, among the hubs are *STAT1*, *STAT3*, *NFKBIA* (*IκBa*), and NFKB1, which are well known to be associated with TLR and IFN signaling pathways[43–48]. ORA of these 34 genes indicates that in addition to dectin-1[49] and NLRs signaling, they mostly enrich both type I and II IFN and

several TLR signaling pathways (TLR1/2, TLR2/6, MyD88, and TRAF6-mediated NF-κB activation) (**Suppl. Fig. 2b-c**).

Common TLR-and IFN-associated DEGs and signaling pathways across microarray, bulk, and single-cell RNA-seq datasets

Finally, we revisited the scRNAseq data and found that 11 TLR- and 23 IFN-associated DEGs are also among those WBCs, PBMCs and moDCs DEGs identified by microarray and bulk RNAseq datasets (**Suppl. Table 13**)**.** Thus, indicating that the network interplay of TLR- and IFN-associated DEGs are not a particular feature of a specific leukocyte cell population since *C. albicans* systemically activated this network throughout the different innate (monocytes, natural killer, and plasmacytoid dendritic cells) and adaptive cells (CD4+, CD8+, and CD19+ lymphocytes) identified by the scRNAseq dataset. **Fig. 8a-b** illustrate these 34 common genes across the leukocytes subpopulations and those present in the WBCs, PBMCs, and moDCs datasets (**Fig. 3a-c**). Hierarchical clustering of common enriched pathways across the cell subpopulations identified by scRNAseq showed a similar up-regulation pattern of TLR- and IFN-associated signaling pathways, forming clusters (**Fig. 8c**), as seen by microarray and bulk RNAseq.

DISCUSSION

The association between PRR activation and cytokine production by immune cells is important for an adequate immune response against pathogens and has been abundantly investigated by linear approaches or strategies designed to identify the anti-fungal

transcriptomic signature[12,24,39,50]. For instance, several immunologic molecules and pathways such as those triggered by TLR and IFN, which induce the generation of T cell subpopulations (e.g., T helper 1 [Th1], Th17, and T regulatory [T reg] cells) have been successfully characterized by individual studies and mechanistic approaches[17]. However, until now, there was no system immunology study to holistically understand the anti-fungal immune responses. Our approach integrates dispersed transcriptomic datasets that investigated the immune response against *C. albicans* and *C. auris,* indicating that the anti-candida immune responses are marked by a previously uncharacterized intricated interferome chain, interconnecting PRR (e.g., CLRs, TLRs, and NLRs) and interleukin (e.g., IFN, TNF, and IL-10) cascades. This immune network is hallmarked by dynamic and consistent crosstalks between the network interplay of TLR and IFN signaling pathways. Besides, we show that there is a consistent overlap between the antiviral and antifungal immune responses, which supports the previously reported pivotal role of IFN type I in the immune response against *C. albicans*[24]. Notably, this immunologic overlap might be not restricted to viral infection. For instance, studies need to be performed to investigate its extension to the anti-*Mycobacteria tuberculosis* immune responses. The host's protection against this intracellular bacterium relies not only on an IFN-γ centered phenomenon but also requires the synergism of type I IFNs and other cytokines such as IL-17[51]. Thus, our results strongly suggest that the immune system employs a multitude of molecules, working as a "social" network, in which cells effectively collaborate and communicate to maintain immunologic homeostasis[52,53].

Our integrative and systems immunology approach provides a transcriptomic landscape of the anti-candida defenses that will contribute to better understand the host

312 immunological dynamics initiated against these fungal pathogens. Since we currently are
313 confronted with increasing numbers of invasive fungal infections, in part due to the
314 emergence of anti-fungal drug resistance, it is imperative to address this global health
315 problem[2,40,54]. Diseases caused by viruses and bacteria have been recognized as important
316 public health issues for centuries, while fungal infections have historically been neglected[55].
317 Numerous transcriptomic, epigenomic, and proteomic data are available that investigate the
318 immune response against viruses and bacteria using public databases[56–58]. However, most
319 investigations addressing the anti-fungal immune response employ linear and mechanistic
320 approaches[15] and there are very limited numbers of publicly available transcriptomic
321 datasets of human immune responses to fungal infections. Most of these studies focus on the
322 transcriptomic response of human immune cells activated with *C. albicans* but only one
323 dataset explores the immune response to *C. auris,* one of the most critical emerging fungal
324 pathogen[39]. The integrative approach we employed was designed to obtain a comprehensive
325 understanding of the anti-fungal immune response.

326 The results of our study provide complementary arguments for linear and mechanistic
327 strategies that confirm a dynamic interplay between TLR and type I and II IFN-associated
328 molecules[59]. It has been suggested that different TLRs synergistically activate immune cells
329 to, for instance, induce the expression of several proinflammatory molecules through the
330 cooperation of NF-κB, IRF, STAT, MAPK, ITAM, and PI3K signaling pathways[60–62]. On the one
331 hand, TLR-induced NF-κB signaling promotes the production of several key cytokines
332 including IFNs that activate STAT1-mediated signaling pathway[63]. On the other hand, IFN-γ
333 increases the expression of genes encoding TLRs[64–67]. IFNs also potentialize TLR-induced
334 gene transcription by creating a primed chromatin environment by histone acetylation that

allows sustained occupancy of transcription factors STAT1 and IRF-1 at promotors and enhancers at the *TNF*, *IL-6,* and *IL12B* loci[68] . Thus, our phenomenological study confirms these previously reported mechanistic studies and provides new insights into the molecular network of TLR and IFN signaling pathways in anti-Candida immune response. These networks also need to be investigated in other mycoses (paracoccidioidomycosis, histoplasmosis, and cryptococcosis) and other neglected diseases (Dengue, Zika, leishmaniasis, and Chagas disease) occurring in developing countries[55]. The TLR and IFN interactome involve more complex events than previously thought, demanding further bottom-up and top-down systems immunology investigations.

Our conclusions are based on the integration of publicly available human transcriptomes that identified common DEGs, as well as biological processes and signaling pathways consistently modulated across several leukocyte subpopulations in response to fungal pathogens (*C. albicans* and *C. auris*). Among these DEGs, we highlight those involved in IFN-α/β (e.g., ISGs, IRFs, SOCS, and GBPs), TLR3,4,7/8,9, and TRAF-mediated NF-κB signaling cascades. The correlation levels of DEGs involved in these signature clusters increased upon stimulation with *C. albicans*. Of note, among the consistently identified DEGs are those previously associated with IEI that increase the host susceptibility to fungal infections such as those causing chronic mucocutaneous candidiasis. Besides, these DEGs are also involved with immunological pathways related to the development of IEI phenocopies such as those targeted by anti-IL-17 or anti-IL17RA autoantibodies that result in increased susceptibility to Candida spp. infections. Because the outcome of fungal infections depends primarily on the host immune response, it is most relevant to review those IEIs that predispose to Candida infections[25,72]. IEIs represent an essential research field that

investigates natural human susceptibility models to infection, often revealing the non-redundant role of genes involved in immunologic homeostasis[73–75]. Of the 416 molecular defined IEI recently summarized by the expert committee of the IUIS, more than 20 syndromes were recognized to be associated with susceptibility to fungal infections[42]. This list of genes associated with increased risk of fungal infections includes genes regulating signaling via the IL-2 receptor, via NF-kB activation, IFN induced signaling, activation of STATs, and TLR signaling. Thus, these observations support the relevance of the interactome and interplay events characterized by our analysis increasing the understanding of consistent immunologic pathways essential for the immune response to Candida infections.

All in all, our work provides a systems immunology view of the interactome of anti-fungal molecules, revealing a consistent network interplay between TLR and IFN signaling pathways in response to *C. albicans* and *C. auris*. This study also indicates new biomarkers and provides novel insights into the systemic immunological mechanism against fungal infections. Future works dissecting this interplay will pave the way for new immunotherapy approaches to reduce the high mortality rate caused by fungal infections. Also, our study indicates that the exploration of functional genomic approaches by applying systems immunology methods to investigate IEI will provide new opportunities to further understand the immune system *in natura*.

ONLINE METHODS

METHODS

Datasets and curation

We performed an integrative analysis by searching on NCBI GEO database[76] and ArrayExpress database[77], to identify publicly available gene expression data of infection by *C. albicans and C. auris* in whole blood, PBMCs, and moDCs. This search comprised studies published between March 2010 and July 2020. Since transcriptome datasets from patients with candidiasis were not publicly available we consider as criteria for inclusion: (1) gene expression data of whole blood, PBMCs, and moDCs of in vitro infection with *C. albicans*; (2) studies composed of at least 2 samples per group; (3) the inclusion of control groups for comparison; (4) all gene expression analysis platforms were considered; and (5) only studies that have provided the transcriptome data were included for the integrative analyses. Our exclusion criteria were (1) non-human samples, (2) treatment before molecular genetic analysis, and (3) review studies. RNAseq and MicroArray studies were included in our integrative analysis, five studies were retrieved from the NCBI GEO database[76] (GSE65088 and GSE114180, GSE42606, GSE154911, and GSE77969) and two from ArrayExpress database[77] (E-MTAB-135, E-MTAB-751). Also, a single-cell RNAseq study was included[78].

Single-cell RNASeq analysis

We obtained the Seurat Object containing the scRNAseq data from De Vries et al. (2020), which was deposited in the single-cell eQTLGen Consortium database (https://eqtlgen.org/candida.html). We followed the default Seurat pipeline (https://satijalab.org/seurat/articles/pbmc3k_tutorial.html) as previously described by Stuart et al.[78] to perform differential expression analysis and data visualization (UMAP, dotplot, and heatmap).

Differential Expression Analysis of bulk RNAseq and microarray data

To characterize the immunological signature from the global transcriptional profiles in infection by *C. albicans*, read counts of each RNAseq study were transformed (log2 count per million), and NetworkAnalyst 3.0 webtool (https://www.networkanalyst.ca/)[79] was used to perform differential expression analysis, applying DESeq2 pipeline. The microarray studies were analyzed through GEO2R web application[80], available at http://www.ncbi.nlm.nih.gov/geo/geo2r/, using limma-voom pipeline[81]. To select the up and downregulated genes between *C. albicans* infection and the normal group, we used the statistical cutoffs of log2 fold-change > 1 (upregulated) or < -1 (downregulated) and adjusted p-value < 0.05.

Analysis of Gene Co-Expression Modules

We selected the dataset GSE42606 to analyze the gene co-expression modules with the R-package CEMiTool 1.12.2 using default parameters[30].

Enrichment Analysis and Data Visualization

We used the differentially expressed genes (DEGs) to identify enriched ontology terms. The pathways and the biological processes were identified through an Over-representation Analysis (ORA) and EnrichR[82], and the significant enriched immunological terms were generated according to adjusted p-value < 0.05. The Upset and Venn Graphs demonstrating the intersections and comparisons between common DEGs among the datasets were generated through the webtool Intervene[83] and Bioinformatics & Evolutionary Genomics

(http://bioinformatics.psb.ugent.be/webtools/Venn/). We plotted the set of genes shared between the dataset in bubble-based heat maps, applying One minus cosine similarity through the webtool Morpheus (https://software.broadinstitute.org/morpheus/)[84]. We used ClusterProfiler[85] to obtain dot plots of enriched terms associated with *C. albicans* and *C. auris* infections. ClusterProfiler and ORA, were performed on R software version 4.0.2 (https://www.r-project.org/index.html), through the packages DOSE, enrichplot, reactomePA, and clusterprofiler[85]. The GOplot was plotted using the R packages unikn, circlize, and GOplot[86]. The statistical graphs were constructed using the functionalities of the ggplot2 package[87]. We represented the shared DEGs between different fungal infections (*C. albicans* and *C. auris*) through circular heatmaps, using the R packages circlize and ComplexHeatmap[88].

Correlation Analysis

We used the GSE42606 dataset to perform the correlation analysis between genes associated with TLRs as well as Type I and II IFN signaling cascades. The correlation matrices were generated with the webtool Intervene[83] (https://intervene.readthedocs.io/en/latest/index.html), using Pearson coefficient. The Canonical Correlation Analysis (CCA)[89] was applied to investigate patterns of association between IFN and TLR genes from the same dataset. The CCA was performed on R software version 4.0.2 (https://www.r-project.org/index.html), through the packages CCA, and whitening[89]. Principal Component Analysis (PCA) analysis was built using R functions prcomp and princomp, through factoextra package.

Molecular Network

Networks of related pathways to fungal infection immune responses and physical protein-protein interaction (PPI) networks of DEGs found across all datasets were annotated, analyzed and visualized using NAViGaTOR 3.0,14[90]. Node color represents Gene Ontology cellular component as per legend. DEGs were used as input into Integrated Interactions Database (IID version 2020-05; http://ophid.utoronto.ca/iid)[91,92] to identify direct physical protein interactions. Networks were exported in SVG file format, and finalized in Adobe Illustrator 2021.

Multi-study Factor Analysis (MSFA)

MSFA is a generalized version of factor analysis that allows for the joint analysis of multiple studies. MSFA estimates shared factors common to all studies, as well as factors specific to individual studies. Estimation of parameters for the MSFA model can be computed using either a frequentist or a Bayesian approach. Compared with the frequentist analysis, the Bayesian offers two major advantages: 1- it provides a better defined factors, and 2- it chooses the dimension of the common and study-specific factors through a practical and useful approach. We adopt the Bayesian multi-study, for the inferential analysis to identify - common and study-specific factors[25,33,93] shared by GSE65088 and GSE42606. The Bayesian MSFA considers all data at once in an integrated approach, estimating parameters by maximum-likelihood analysis[94].

Interferome Analysis

The identification of interferome genes was performed with Interferome V2.01 (http://www.interferome.org/interferome/home.jspx).

Single-cell RNA-seq differential expression analysis

Seurat package was used to obtain the DEGs between the different cell types under the conditions of infection by *C. albicans* and resting cells. Enrichment of DEGs by cell group and by total DEGs was done according to the described for ClusterProfiler package.

Code Availability

R codes used in this work are available

athttps://github.com/ranieri131/SalgadoRC_CANDIDA_IMMUNE_RESPONSE_2021

Acknowledgments

We acknowledge the São Paulo Research Foundation (FAPESP grants 2018/18886-9, 2020/01688-0, and 2020/07069-0 to OCM) for financial support. RCS is financed by the national council for scientific and technological development (CNPQ). Computational analysis was supported by FAPESP and partially by the grants from Ontario Research Fund (#34876), Natural Sciences Research Council (NSERC #203475), Canada Foundation for Innovation (CFI #29272, #225404, #33536), and IBM. This study was financed in part by the coordination for the improvement of higher education personnel – Brazil (CAPES) – finance code 001.

Author Contributions

RCS, PPF, OCM co-wrote the manuscript; RCS, DLMF, TTF, PPF, NOSC, VLGC, LFS, OCM provided scientific insights; RCS, DLMF, AHCM, SMSN, KTA, CASP, GCB, DRP, ISF, RV, IJ, and OCM performed bioinformatics analyses; RCS, DLMF, and OCM conceived and designed the study; RCS, TTF, LFS, PPF, NOSC, VLGC, HDO, LFS, IJ, ACN, and OCM revised and edited the final manuscript; ACN and OCM supervised the project.

Competing interest statement

The authors declare no competing financial and/or non-financial interests concerning the work described.

Data availability

The published transcriptome datasets can be found in the GEO and Array Express databases (IDs. GSE65088, GSE114180, GSE42606, GSE154911, GSE77969, E-MTAB-135, E-MTAB-751). Single-cell data is available as Seurat Object on doi.org/10.1371/journal.ppat.1008408.

REFERENCES

1. Chow, N. A. *et al.* Multiple introductions and subsequent transmission of multidrug-resistant Candida auris in the USA: a molecular epidemiological survey. *Lancet Infect. Dis.* **18**, 1377–1384 (2018).
2. GLASS | World Health Organization. *WHO* (2018).
3. Casadevall, A. Don't Forget the Fungi When Considering Global Catastrophic Biorisks. *Health Security* vol. 15 341–342 (2017).
4. Warnock, D. W. Fungal diseases: An evolving public health challenge. *Med. Mycol.* **44**, 697–705 (2006).
5. Meis, J. F. & Chowdhary, A. Candida auris: a global fungal public health threat. *The Lancet Infectious Diseases* vol. 18 1298–1299 (2018).
6. Guinea, J. Global trends in the distribution of Candida species causing candidemia. *Clinical Microbiology and Infection* vol. 20 5–10 (2014).
7. Bongomin, F., Gago, S., Oladele, R. O. & Denning, D. W. Global and multi-national prevalence of fungal diseases—estimate precision. *Journal of Fungi* vol. 3 (2017).
8. Zeng, Z. R. *et al.* Surveillance study of the prevalence, species distribution, antifungal susceptibility, risk factors and mortality of invasive candidiasis in a tertiary teaching hospital in Southwest China. *BMC Infect. Dis.* **19**, 939 (2019).
9. Kullberg, B. J. & Arendrup, M. C. Invasive Candidiasis. *N. Engl. J. Med.* **373**, 1445–1456 (2015).
10. Lee, P. P. & Lau, Y.-L. Cellular and Molecular Defects Underlying Invasive Fungal Infections-Revelations from Endemic Mycoses. *Front. Immunol.* **8**, 735 (2017).
11. Cheng, S. C., Joosten, L. A. B., Kullberg, B. J. & Netea, M. G. Interplay between Candida albicans and the mammalian innate host defense. *Infection and Immunity* vol. 80 1304–1313 (2012).
12. Muñoz, J. F. *et al.* Coordinated host-pathogen transcriptional dynamics revealed using sorted subpopulations and single macrophages infected with Candida albicans. *Nat. Commun.* **10**, 1607 (2019).
13. Johnson, M. D. *et al.* Cytokine gene polymorphisms and the outcome of invasive candidiasis: A prospective cohort study. *Clin. Infect. Dis.* **54**, 502–510 (2012).
14. Smeekens, S. P. *et al.* Functional genomics identifies type i interferon pathway as central for host defense against Candida albicans. *Nat. Commun.* **4**, 1342 (2013).
15. Romani, L. Immunity to fungal infections. *Nature Reviews Immunology* vol. 11 275–288 (2011).
16. Patin, E. C., Thompson, A. & Orr, S. J. Pattern recognition receptors in fungal immunity. *Seminars in Cell and Developmental Biology* vol. 89 24–33 (2019).
17. Netea, M. G., Joosten, L. A. B., Van Der Meer, J. W. M., Kullberg, B. J. & Van De Veerdonk, F. L. Immune defence against Candida fungal infections. *Nature Reviews Immunology* vol. 15 630–642 (2015).

18. Liu, T., Zhang, L., Joo, D. & Sun, S. C. NF-κB signaling in inflammation. *Signal Transduction and Targeted Therapy* vol. 2 1–9 (2017).

19. Warnatsch, A. *et al.* Reactive Oxygen Species Localization Programs Inflammation to Clear Microbes of Different Size. *Immunity* **46**, 421–432 (2017).

20. Kolaczkowska, E. & Kubes, P. Neutrophil recruitment and function in health and inflammation. *Nature Reviews Immunology* vol. 13 159–175 (2013).

21. Urban, C. F., Reichard, U., Brinkmann, V. & Zychlinsky, A. Neutrophil extracellular traps capture and kill Candida albicans and hyphal forms. *Cell. Microbiol.* **8**, 668–676 (2006).

22. Romani, L. Immunity to fungal infections. *Nat. Rev. Immunol.* **4**, 1–23 (2004).

23. Schimke, L. F. *et al.* Paracoccidioidomycosis Associated With a Heterozygous STAT4 Mutation and Impaired IFN-γ Immunity. *J. Infect. Dis.* **216**, 1623–1634 (2017).

24. Smeekens, S. P. *et al.* Functional genomics identifies type i interferon pathway as central for host defense against Candida albicans. *Nat. Commun.* **4**, 1–10 (2013).

25. Netea, M. G., Joosten, L. A. B., Van Der Meer, J. W. M., Kullberg, B. J. & Van De Veerdonk, F. L. Immune defence against Candida fungal infections. *Nature Reviews Immunology* vol. 15 630–642 (2015).

26. Crosstalk Between IFN- and TLR. *Sci. Signal.* **2006**, tw129–tw129 (2006).

27. Chaussabel, D. & Baldwin, N. Democratizing systems immunology with modular transcriptional repertoire analyses. *Nature Reviews Immunology* vol. 14 271–280 (2014).

28. Smeekens, S. P. *et al.* Functional genomics identifies type i interferon pathway as central for host defense against Candida albicans. *Nat. Commun.* **4**, 1–10 (2013).

29. WGCNA package: Frequently Asked Questions. https://horvath.genetics.ucla.edu/html/CoexpressionNetwork/Rpackages/WGCNA/faq.html.

30. Russo, P. S. T. *et al.* CEMiTool: a Bioconductor package for performing comprehensive modular co-expression analyses. *BMC Bioinformatics* **19**, 56 (2018).

31. Yu, G., Wang, L. G., Han, Y. & He, Q. Y. ClusterProfiler: An R package for comparing biological themes among gene clusters. *Omi. A J. Integr. Biol.* **16**, 284–287 (2012).

32. Ramesh, N., Salama, M., Dangott, B. & Tasdizen, T. Isolation and two-step classification of normal white blood cells in peripheral blood smears. *J. Pathol. Inform.* **3**, 13 (2012).

33. De Vito, R., Bellio, R., Trippa, L. & Parmigiani, G. Multi-study factor analysis. *Biometrics* **75**, 337–346 (2019).

34. Romani, L. Immunity to fungal infections. *Nature Reviews Immunology* vol. 11 275–288 (2011).

35. Romani, L. & Puccetti, P. Controlling pathogenic inflammation to fungi. *Expert Review of Anti-Infective Therapy* vol. 5 1007–1017 (2007).

36. Fallarino, F., Puccetti, P., Romani, L., Zelante, T. & De Luca, A. Pathogenic

Inflammation to Fungi IL-17 and Therapeutic Kynurenines in. *J Immunol Ref.* **180**, 5157–5162 (2008).

37. Aggarwal, R. & Ranganathan, P. Common pitfalls in statistical analysis: The use of correlation techniques. *Perspect. Clin. Res.* **7**, 187 (2016).

38. Rickman, J. M., Wang, Y., Rollett, A. D., Harmer, M. P. & Compson, C. Data analytics using canonical correlation analysis and Monte Carlo simulation. *npj Comput. Mater.* **3**, 26 (2017).

39. Bruno, M. *et al.* Transcriptional and functional insights into the host immune response against the emerging fungal pathogen Candida auris. *Nat. Microbiol.* **5**, 1516–1531 (2020).

40. Arendrup, M. C. & Patterson, T. F. Multidrug-resistant candida: Epidemiology, molecular mechanisms, and treatment. *J. Infect. Dis.* **216**, S445–S451 (2017).

41. Vallabhajosyula, R. R., Chakravarti, D., Lutfeali, S., Ray, A. & Raval, A. Identifying Hubs in Protein Interaction Networks. *PLoS One* **4**, e5344 (2009).

42. Tangye, S. G. *et al.* Human Inborn Errors of Immunity: 2019 Update on the Classification from the International Union of Immunological Societies Expert Committee. *J. Clin. Immunol.* **40**, 24–64 (2020).

43. Kawai, T. & Akira, S. Signaling to NF-κB by Toll-like receptors. *Trends in Molecular Medicine* vol. 13 460–469 (2007).

44. Tsai, M. H., Pai, L. M. & Lee, C. K. Fine-tuning of type I interferon response by STAT3. *Frontiers in Immunology* vol. 10 1448 (2019).

45. Balic, J. J. *et al.* STAT3 serine phosphorylation is required for TLR4 metabolic reprogramming and IL-1β expression. *Nat. Commun.* **11**, 1–11 (2020).

46. Luu, K. *et al.* STAT1 plays a role in TLR signal transduction and inflammatory responses. *Immunol. Cell Biol.* **92**, 761–769 (2014).

47. Ramana, C. V., Gil, M. P., Schreiber, R. D. & Stark, G. R. Stat1-dependent and -independent pathways in IFN-γ-dependent signaling. *Trends in Immunology* vol. 23 96–101 (2002).

48. Rhee, S. H., Jones, B. W., Toshchakov, V., Vogel, S. N. & Fenton, M. J. Toll-like receptors 2 and 4 activate STAT1 serine phosphorylation by distinct mechanisms in macrophages. *J. Biol. Chem.* **278**, 22506–22512 (2003).

49. Hardison, S. E. & Brown, G. D. C-type lectin receptors orchestrate antifungal immunity. *Nature Immunology* vol. 13 817–822 (2012).

50. Qiao, Y. *et al.* Article Synergistic Activation of Inflammatory Cytokine Genes by Interferon-g-Induced Chromatin Remodeling and Toll-like Receptor Signaling. *Immunity* **39**, 454–469 (2013).

51. Mourik, B. C., Lubberts, E., de Steenwinkel, J. E. M., Ottenhoff, T. H. M. & Leenen, P. J. M. Interactions between type 1 interferons and the Th17 response in tuberculosis: Lessons learned from autoimmune diseases. *Frontiers in Immunology* vol. 8 294 (2017).

52. Rieckmann, J. C. *et al.* Social network architecture of human immune cells unveiled by quantitative proteomics. *Nat. Immunol.* **18**, 583–593 (2017).

53. Bergthaler, A. & Menche, J. The immune system as a social network. *Nature Immunology* vol. 18 481–482 (2017).

54. Perlin, D. S., Rautemaa-Richardson, R. & Alastruey-Izquierdo, A. The global problem of antifungal resistance: prevalence, mechanisms, and management. *The Lancet Infectious Diseases* vol. 17 e383–e392 (2017).

55. Rodrigues, M. L. & Nosanchuk, J. D. Fungal diseases as neglected pathogens: A wake-up call to public health officials. *PLoS Negl. Trop. Dis.* **14**, (2020).

56. PRIDE - Proteomics Identification Database. https://www.ebi.ac.uk/pride/.

57. ArrayExpress < EMBL-EBI. https://www.ebi.ac.uk/arrayexpress/.

58. Home - GEO - NCBI. https://www.ncbi.nlm.nih.gov/geo/.

59. Zhao, J. *et al.* IRF-8/interferon (IFN) consensus sequence-binding protein is involved in toll-like receptor (TLR) signaling and contributes to the cross-talk between TLR and IFN-γ signaling pathways. *J. Biol. Chem.* **281**, 10073–10080 (2006).

60. Hu, X., Chen, J., Wang, L. & Ivashkiv, L. B. Crosstalk among Jak-STAT, Toll-like receptor, and ITAM-dependent pathways in macrophage activation. *J. Leukoc. Biol.* **82**, 237–243 (2007).

61. Bohnenkamp, H. R., Papazisis, K. T., Burchell, J. M. & Taylor-Papadimitriou, J. Synergism of Toll-like receptor-induced interleukin-12p70 secretion by monocyte-derived dendritic cells is mediated through p38 MAPK and lowers the threshold of T-helper cell type I responses. *Cell. Immunol.* **247**, 72–84 (2007).

62. Makela, S. M., Strengell, M., Pietila, T. E., Osterlund, P. & Julkunen, I. Multiple signaling pathways contribute to synergistic TLR ligand-dependent cytokine gene expression in human monocyte-derived macrophages and dendritic cells. *J. Leukoc. Biol.* **85**, 664–672 (2009).

63. Tong, Y. *et al.* Enhanced TLR-induced NF-κB signaling and type I interferon responses in NLRC5 deficient mice. *Cell Res.* **22**, 822–835 (2012).

64. Bosisio, D. *et al.* Stimulation of toll-like receptor 4 expression in human mononuclear phagocytes by interferon-γ: A molecular basis for priming and synergism with bacterial lipopolysaccharide. *Blood* **99**, 3427–3431 (2002).

65. Schroder, K. *et al.* PU.1 and ICSBP control constitutive and IFN-γ-regulated Tlr9 gene expression in mouse macrophages . *J. Leukoc. Biol.* **81**, 1577–1590 (2007).

66. Kajita, A. *et al.* Interferon-Gamma Enhances TLR3 Expression and Anti-Viral Activity in Keratinocytes. *J. Invest. Dermatol.* **135**, 2005–2011 (2015).

67. Mita, Y. *et al.* Toll-like receptor 4 surface expression on human monocytes and B cells is modulated by IL-2 and IL-4. *Immunol. Lett.* **81**, 71–75 (2002).

68. Qiao, Y. *et al.* Synergistic activation of inflammatory cytokine genes by interferon-γ-induced chromatin remodeling and toll-like receptor signaling. *Immunity* **39**, 454–469 (2013).

69. GLASS | World Health Organization. *WHO* (2018).

70. Chow, N. A. *et al.* Multiple introductions and subsequent transmission of multidrug-resistant Candida auris in the USA: a molecular epidemiological survey. *Lancet Infect. Dis.* **18**, 1377–1384 (2018).

71. Bousfiha, A. *et al.* Human Inborn Errors of Immunity: 2019 Update of the IUIS Phenotypical Classification. *J. Clin. Immunol.* **40**, 66–81 (2020).

72. Muñoz, J. F. *et al.* Coordinated host-pathogen transcriptional dynamics revealed using sorted subpopulations and single macrophages infected with Candida albicans. *Nat. Commun.* **10**, 1–15 (2019).

73. Casanova, J.-L. & Abel, L. Lethal Infectious Diseases as Inborn Errors of Immunity: Toward a Synthesis of the Germ and Genetic Theories. *Annu. Rev. Pathol. Mech. Dis.* **16**, (2021).

74. Notarangelo, L. D., Bacchetta, R., Casanova, J. L. & Su, H. C. Human inborn errors of immunity: An expanding universe. *Science Immunology* vol. 5 (2020).

75. Casanova, J. L. & Abel, L. The human model: A genetic dissection of immunity to infection in natural conditions. *Nature Reviews Immunology* vol. 4 55–66 (2004).

76. Edgar, R., Domrachev, M. & Lash, A. E. Gene Expression Omnibus: NCBI gene expression and hybridization array data repository. *Nucleic Acids Res.* **30**, 207–210 (2002).

77. Athar, A. *et al.* ArrayExpress update - from bulk to single-cell expression data. *Nucleic Acids Res.* **47**, D711–D715 (2019).

78. de Vries, D. H. *et al.* Integrating GWAS with bulk and single-cell RNA-sequencing reveals a role for LY86 in the anti-Candida host response. *PLoS Pathog.* **16**, (2020).

79. Zhou, G. *et al.* NetworkAnalyst 3.0: A visual analytics platform for comprehensive gene expression profiling and meta-analysis. *Nucleic Acids Res.* **47**, W234–W241 (2019).

80. Barrett, T. *et al.* NCBI GEO: archive for functional genomics data sets—update. *Nucleic Acids Res.* **41**, D991–D995 (2012).

81. Law, C. W., Chen, Y., Shi, W. & Smyth, G. K. Voom: Precision weights unlock linear model analysis tools for RNA-seq read counts. *Genome Biol.* **15**, R29 (2014).

82. Kuleshov, M. V. *et al.* Enrichr: a comprehensive gene set enrichment analysis web server 2016 update. *Nucleic Acids Res.* **44**, W90–W97 (2016).

83. Khan, A. & Mathelier, A. Intervene: a tool for intersection and visualization of multiple gene or genomic region sets. *BMC Bioinformatics* **18**, 287 (2017).

84. Starruß, J., de Back, W., Brusch, L. & Deutsch, A. Morpheus: a user-friendly modeling environment for multiscale and multicellular systems biology. *Bioinformatics* **30**, 1331–2 (2014).

85. Yu, G., Wang, L. G., Han, Y. & He, Q. Y. ClusterProfiler: An R package for comparing biological themes among gene clusters. *Omi. A J. Integr. Biol.* **16**, 284–287 (2012).

86. Walter, W., Sánchez-Cabo, F. & Ricote, M. GOplot: an R package for visually combining expression data with functional analysis: Fig. 1. *Bioinformatics* **31**, 2912–2914 (2015).

87. Wickham, H. Getting Started with ggplot2. in 11–31 (2016). doi:10.1007/978-3-319-24277-4_2.

88. Gu, Z., Eils, R. & Schlesner, M. Complex heatmaps reveal patterns and correlations in multidimensional genomic data. *Bioinformatics* **32**, 2847–2849 (2016).

89. Jendoubi, T. & Strimmer, K. A whitening approach to probabilistic canonical correlation analysis for omics data integration. *BMC Bioinformatics* **20**, 15 (2019).

90. Brown, K. R. *et al.* NAViGaTOR: Network Analysis, Visualization and Graphing Toronto. *Bioinformatics* **25**, 3327–3329 (2009).

91. Kotlyar, M., Pastrello, C., Malik, Z. & Jurisica, I. IID 2018 update: Context-specific physical protein-protein interactions in human, model organisms and domesticated species. *Nucleic Acids Res.* **47**, D581–D589 (2019).

92. Pastrello, C., Kotlyar, M. & Jurisica, I. Informed use of protein–protein interaction data: A focus on the integrated interactions database (IID). in *Methods in Molecular Biology* vol. 2074 125–134 (Humana Press Inc., 2020).

93. Cabral-Marques, O. *et al.* GPCR-specific autoantibody signatures are associated with physiological and pathological immune homeostasis. *Nat. Commun.* **9**, 5224 (2018).

94. Dempster, A. P., Dempster, A. P., Laird, N. M. & Rubin, D. B. Maximum likelihood from incomplete data via the EM algorithm. *J. R. Stat. Soc. Ser. B* **39**, 1--38 (1977).

95. Toshchakov, V. *et al.* TLR4, but not TLR2, mediates IFN-β-induced STATIα/β-dependent gene expression in macrophages. *Nat. Immunol.* **3**, 392–398 (2002).

96. Zhao, L. J., Hua, X., He, S. F., Ren, H. & Qi, Z. T. Interferon alpha regulates MAPK and STAT1 pathways in human hepatoma cells. *Virol. J.* **8**, 157 (2011).

97. Valledor, A. F. *et al.* Selective Roles of MAPKs during the Macrophage Response to IFN-γ. *J. Immunol.* **180**, 4523–4529 (2008).

98. Pfeffer, L. M. The role of nuclear factor κb in the interferon response. *Journal of Interferon and Cytokine Research* vol. 31 553–559 (2011).

99. Iwanaszko, M. & Kimmel, M. NF-κB and IRF pathways: cross-regulation on target genes promoter level. *BMC Genomics* **16**, 307 (2015).

100. Antonczyk, A. *et al.* Direct inhibition of IRF-dependent transcriptional regulatory mechanisms associated with disease. *Front. Immunol.* **10**, 1176 (2019).

101. Miettinen, M., Sareneva, T., Julkunen, I. & Matikainen, S. IFNs activate toll-like receptor gene expression in viral infections. *Genes Immun.* **2**, 349–355 (2001).

Graphic abstract

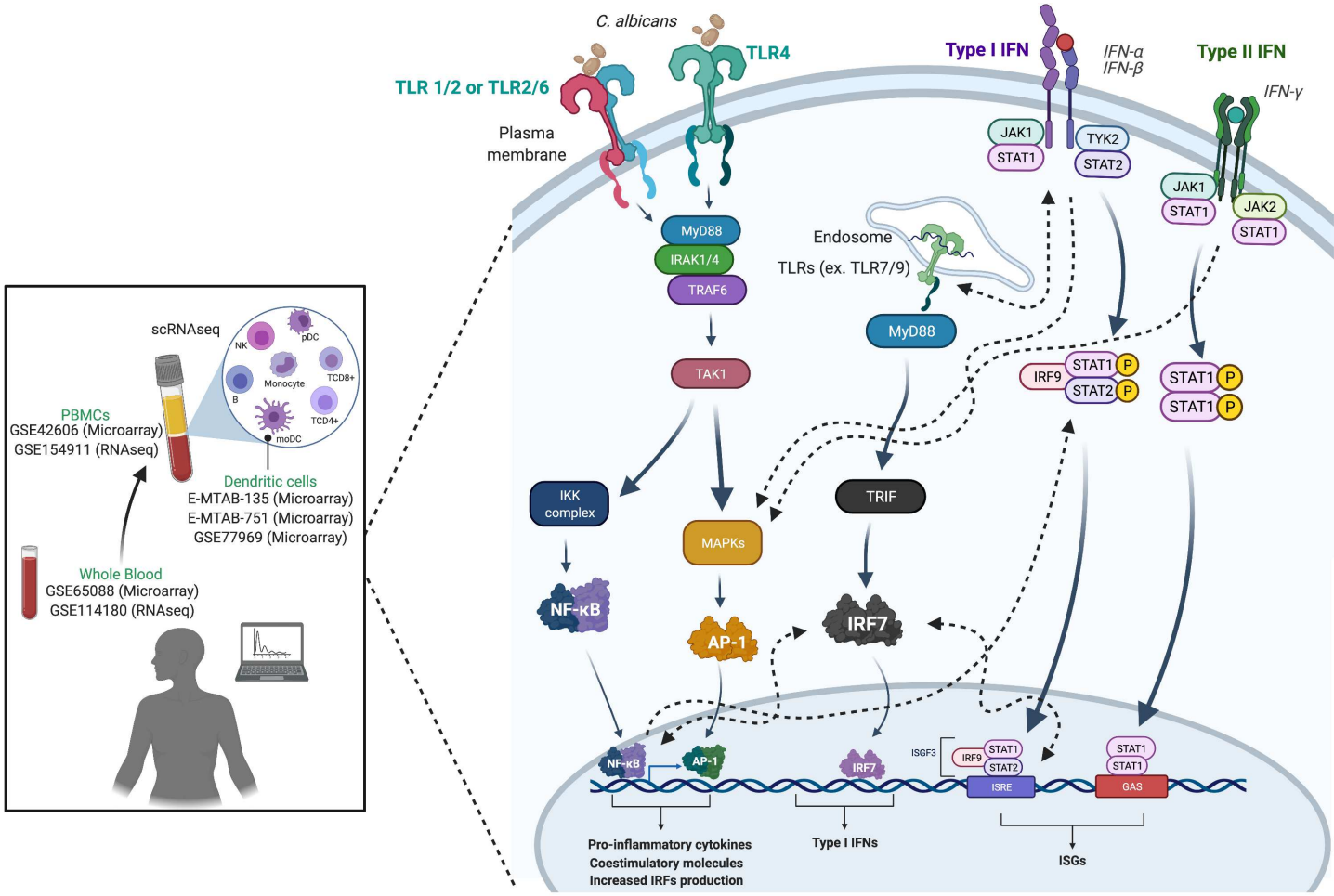

Graphic abstract. Schematic view summarizing datasets and the interplay between TLR and IFN signaling pathways (based on references [48,95–101]) in the immune response to *C. albicans* (created using BioRender.com). *IFN, Interferon; TLR, Toll-like Receptor.*

Figure 1

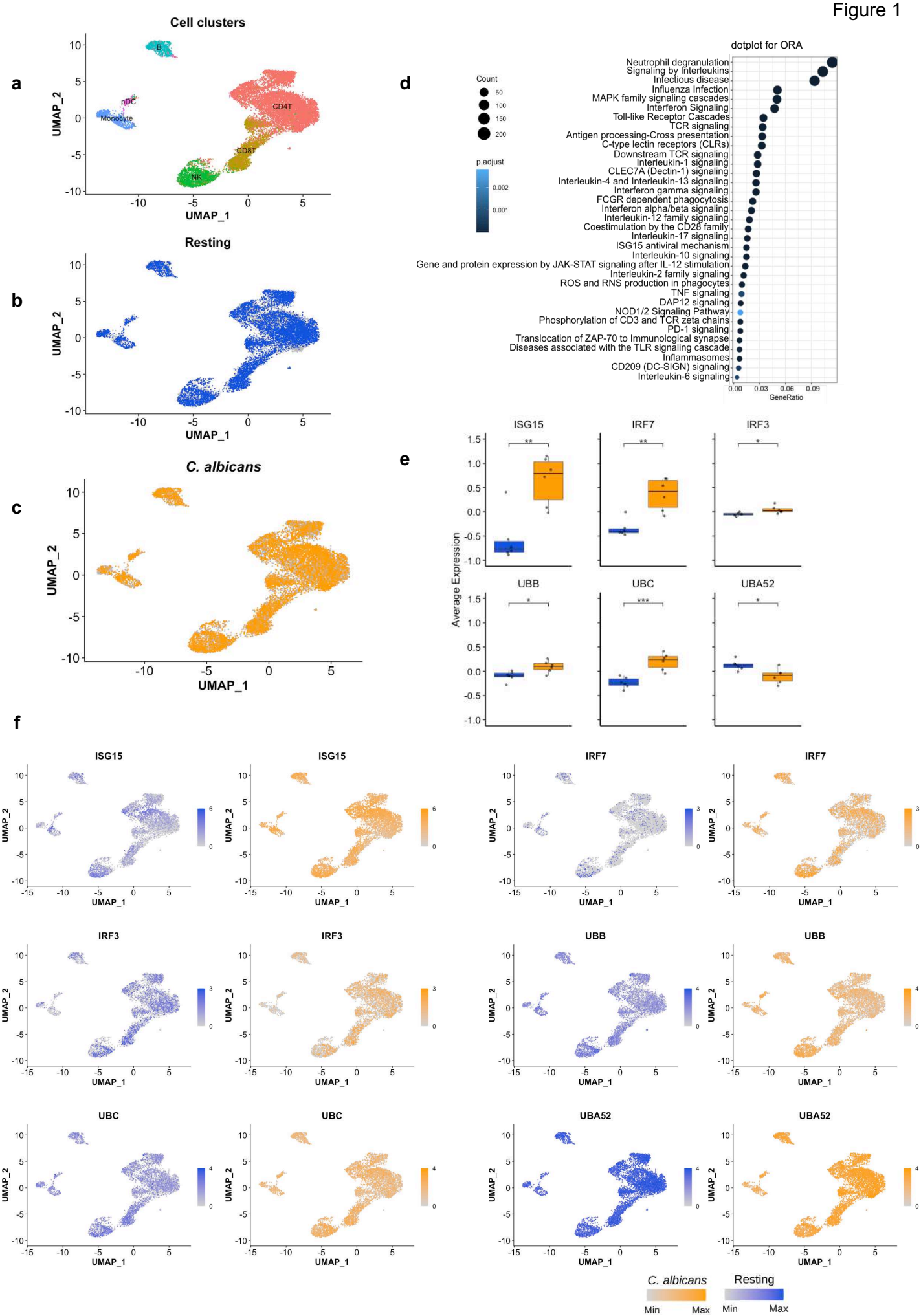
a
Cell clusters
B
pDC
Monocyte
CD4T
CD8T
NK
UMAP_2
UMAP_1
b
Resting
c
C. albicans
d
dotplot for ORA
Count
50
100
150
200
p.adjust
0.002
0.001
Neutrophil degranulation
Signaling by Interleukins
Infectious disease
Influenza Infection
MAPK family signaling cascades
Interferon Signaling
Toll-like Receptor Cascades
TCR signaling
Antigen processing-Cross presentation
C-type lectin receptors (CLRs)
Downstream TCR signaling
Interleukin-1 signaling
CLEC7A (Dectin-1) signaling
Interleukin-4 and Interleukin-13 signaling
Interferon gamma signaling
FCGR dependent phagocytosis
Interferon alpha/beta signaling
Interleukin-12 family signaling
Coestimulation by the CD28 family
Interleukin-17 signaling
ISG15 antiviral mechanism
Interleukin-10 signaling
Gene and protein expression by JAK-STAT signaling after IL-12 stimulation
Interleukin-2 family signaling
ROS and RNS production in phagocytes
TNF signaling
DAP12 signaling
NOD1/2 Signaling Pathway
Phosphorylation of CD3 and TCR zeta chains
PD-1 signaling
Translocation of ZAP-70 to Immunological synapse
Diseases associated with the TLR signaling cascade
Inflammasomes
CD209 (DC-SIGN) signaling
Interleukin-6 signaling
GeneRatio
e
ISG15
IRF7
IRF3
UBB
UBC
UBA52
Average Expression
f
C. albicans
Min
Max
Resting
Min
Max

Fig. 1. scRNAseq revealed common activation of TLR and IFN signaling pathways. a, UMAP visualization of scRNAseq profiles colored according to cell clusters. **b, c,** UMAP of resting and *C. albicans*-activated cells groups. **d**, Dot plot showing pathways associated with immune response to *C. albicans*, obtained by ORA of DEGs. **e,** Boxplot and **f,** UMAP of DEGs associated with both TLR and IFN signaling pathways, additional DEGs associated with these two pathways are described in **Suppl. Table 3**. *DEGs, Differentially Expressed Genes*; *IFN, Interferon; ORA, Over representation analysis; scRNAseq, single-cell RNA sequencing; TLR, Toll-like Receptor; UMAP, Uniform Manifold Approximation and Projection.*


a
Resting
C. albicans
M7
M10
M3
M6
M13
M5
M9
M8
M4
M11
M1
M2
NES
2
1
0
-1
-2
b
FBXO6
LMNA
CSNK2B
MYC
OAS3
PSMA3
DDX60
EIF2AK2
UBC
GAPDH
SAMD9L
RPS6KA1
VIM
Hub
Co-expression
Co-expression + Interaction
Interaction
Degree
200
400
600
c
M1
Interferon Signaling
Signaling by Interleukins
Neutrophil degranulation
RIPK-mediated regulated necrosis
DDX58/IFIH1-mediated induction of interferon-alpha...
Growth hormone receptor signaling
Caspase activation via extrinsic apoptotic signall...
Toll-like Receptor Cascades
Butyrate Response Factor 1 (BRF1) binds and destab...
Class I MHC mediated antigen processing & presenta...
0
5
10
15
20
5
4
3
2
-log10 adj. pvalue
d
EIF1B
CDKN1A
NFKB1
DYNLL1
RIPK2
ETS2
NFKBIA
EGR1
HSPA1A
JUN
F3
BAG3
FYN
IRAK2
UBC
Hub
Co-expression
Interaction
Degree
100
200
300
400
e
M2
Signaling by Interleukins
Toll-like Receptor Cascades
Nucleotide-binding domain, leucine rich repeat con
TNF signaling
Detoxification of Reactive Oxygen Species
Costimulation by the CD28 family
Diseases associated with the TLR signaling cascades
Cellular Senescence
Interferon Signaling
Regulation of lipid metabolism by Peroxisome proli...
0
5
10
15
5
4
3
2
-log10 adj. pvalue

Fig. 2. Modular gene co-expression analysis and the association of TLR and IFN signaling pathways. a, Co-expression modules significantly enriched (M1-M11, and M13) in PBMCs (resting n= 30; *C. albicans* infected n= 24; dataset GSE42606)**. b** and **d** Network representation of M1 and M2 with hubs (most connected genes) colored based on co-expression (blue color), co-expressed and interactions (green color), or only interactions (dark-red color). **c** and **e,** Enrichment representation obtained by modular genes co-expression in M1 and M2 showing significantly (-Log10 transformed adjusted p-value) enriched signaling pathways. *IFN, Interferon; TLR, Toll-like Receptor.*

Figure 3

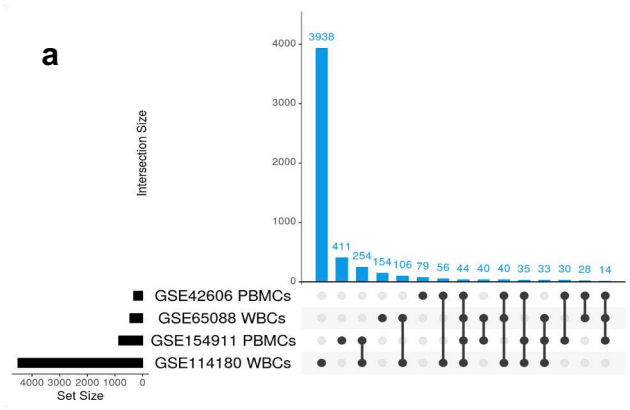
a
Intersection Size
3938
411
254
154
106
79
56
44
40
40
35
33
30
28
14
GSE42606 PBMCs
GSE65088 WBCs
GSE154911 PBMCs
GSE114180 WBCs
Set Size

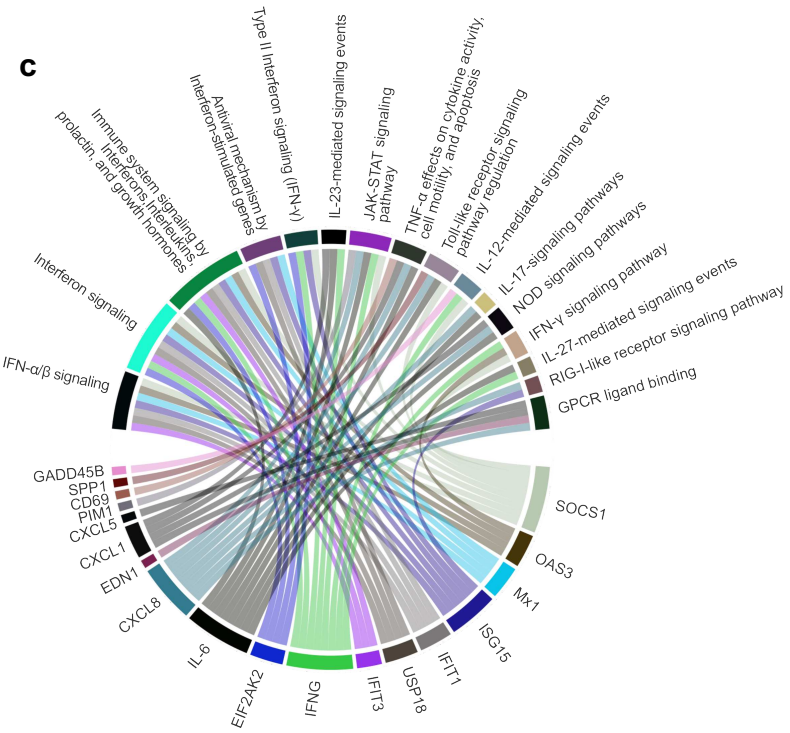
c
Type II Interferon signaling (IFN-γ)
IL-23-mediated signaling events
JAK-STAT signaling pathway
TNF-α effects on cytokine activity, cell motility, and apoptosis
Toll-like receptor signaling pathway regulation
IL-12-mediated signaling events
IL-17-signaling pathways
NOD signaling pathways
IFN-γ signaling pathway
IL-27-mediated signaling events
RIG-I-like receptor signaling pathway
GPCR ligand binding
Antiviral mechanism by Interferon-stimulated genes
Immune system signaling by Interferons, Interleukins, prolactin, and growth hormones
Interferon signaling
IFN-α/β signaling
GADD45B
SPP1
CD69
PIM1
CXCL5
CXCL1
EDN1
CXCL8
IL-6
EIF2AK2
IFNG
IFIT3
USP18
IFIT1
ISG15
Mx1
OAS3
SOCS1

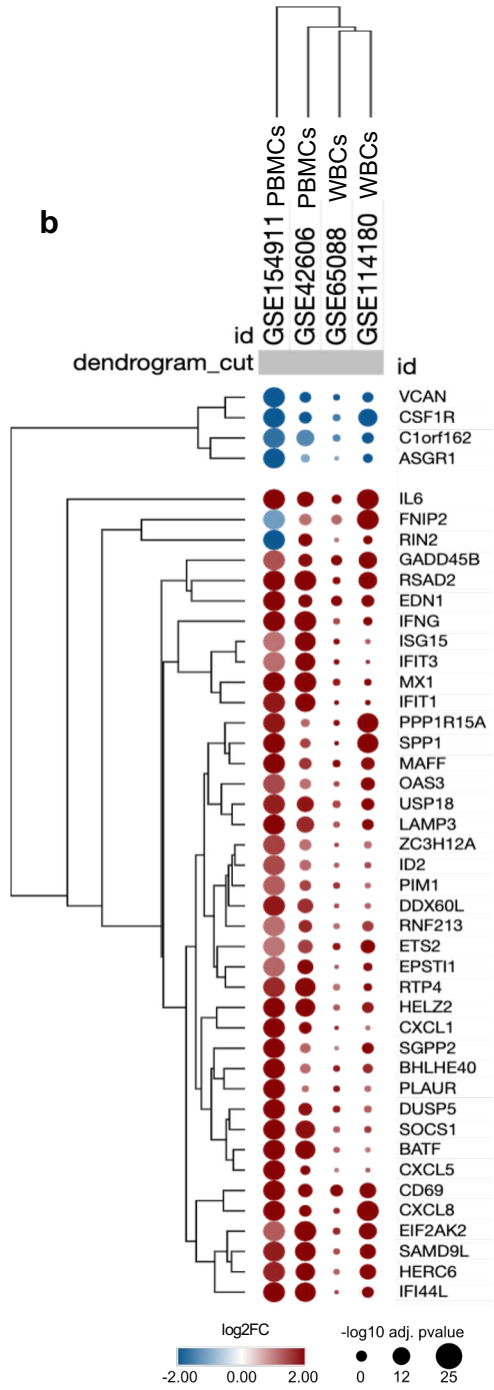
b
id
GSE154911 PBMCs
GSE42606 PBMCs
GSE65088 WBCs
GSE114180 WBCs
dendrogram_cut
id
VCAN
CSF1R
C1orf162
ASGR1
IL6
FNIP2
RIN2
GADD45B
RSAD2
EDN1
IFNG
ISG15
IFIT3
MX1
IFIT1
PPP1R15A
SPP1
MAFF
OAS3
USP18
LAMP3
ZC3H12A
ID2
PIM1
DDX60L
RNF213
ETS2
EPSTI1
RTP4
HELZ2
CXCL1
SGPP2
BHLHE40
PLAUR
DUSP5
SOCS1
BATF
CXCL5
CD69
CXCL8
EIF2AK2
SAMD9L
HERC6
IFI44L
log2FC
-2.00
0.00
2.00
-log10 adj. pvalue
0
12
25

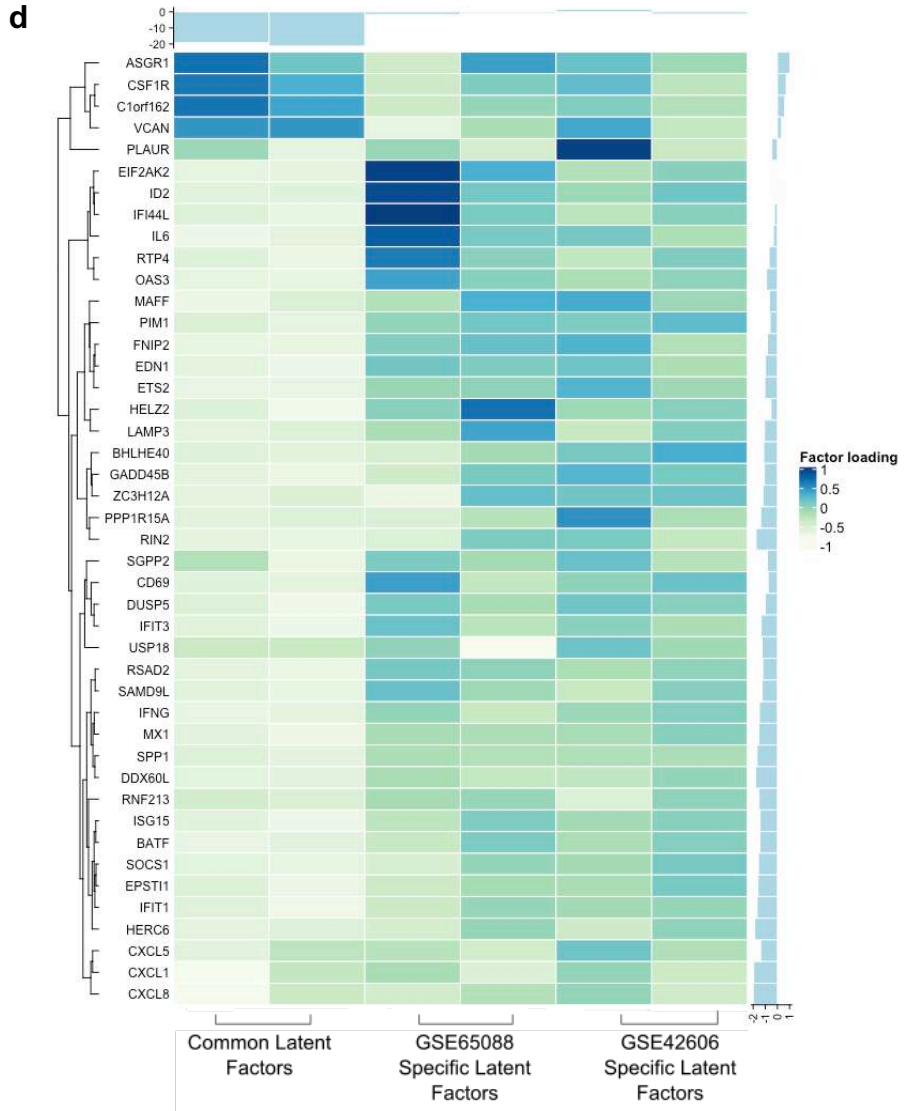
d
0
-10
-20
ASGR1
CSF1R
C1orf162
VCAN
PLAUR
EIF2AK2
ID2
IFI44L
IL6
RTP4
OAS3
MAFF
PIM1
FNIP2
EDN1
ETS2
HELZ2
LAMP3
BHLHE40
GADD45B
ZC3H12A
PPP1R15A
RIN2
SGPP2
CD69
DUSP5
IFIT3
USP18
RSAD2
SAMD9L
IFNG
MX1
SPP1
DDX60L
RNF213
ISG15
BATF
SOCS1
EPSTI1
IFIT1
HERC6
CXCL5
CXCL1
CXCL8
Factor loading
1
0.5
0
-0.5
-1
Common Latent Factors
GSE65088 Specific Latent Factors
GSE42606 Specific Latent Factors

Fig. 3. *C. albicans* activates common TLR- and IFN-associated genes in peripheral blood leukocytes. a, The upset plot displays the number (set size) of DEGs present in each dataset (y-axis: WBCs, GSE65088, and GSE114180; PBMCs: GSE42606 and GSE154911) and their intersections. Black bubbles, present in the rows, mark the dataset which refers to the amount present in the blue columns, with intersections between two or more groups being shown. **b,** Hierarchical clustering of the 44 common DEGs demonstrating gene expression patterns across the different studies. The size and color of circles correspond to -Log10 transformed adjusted p-value and Log2 fold change (Log2FC), respectively. Blue represents downregulated and red indicates up-regulated DEGs. The cut-off applied to identify the down-/upregulated genes was Log2FC < -1/> 1 and adjusted p-value < 0.05. Rows and columns were clustered based on cosine similarity between Log2FC values. **c,** GOplot of selected immunological pathways and associated gene. **d,** Heatmap of common and specific latent factors across the studies. Heatmaps contain genes presenting positive and negative loadings ranging from -1 to 1. *DEGs, Differentially Expressed Genes; PBMCs, Peripheral Blood Mononuclear Cells; WBCs, White Blood Cells.*

Figure 4

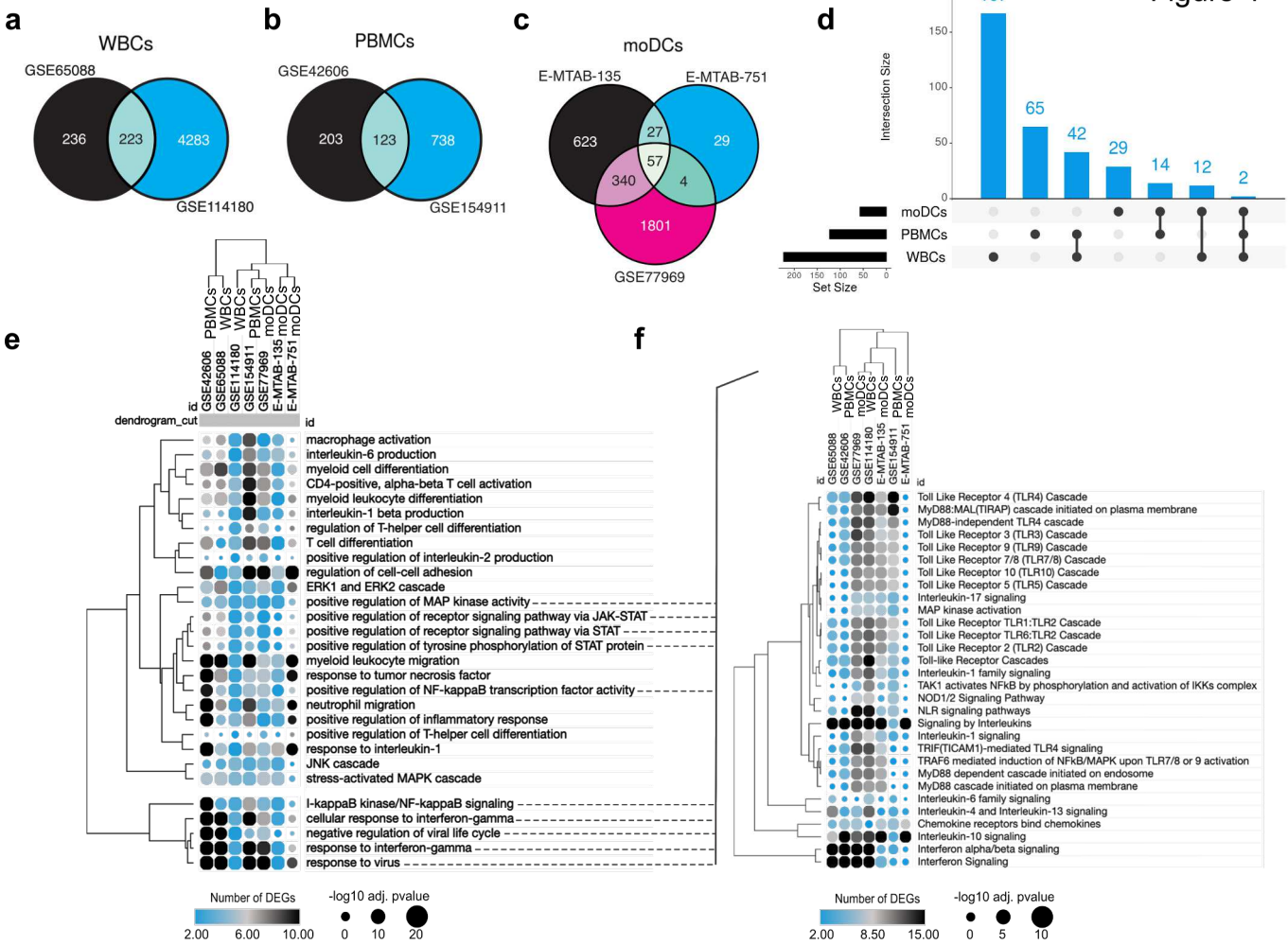
a
WBCs
GSE65088
236
223
4283
GSE114180
b
PBMCs
GSE42606
203
123
738
GSE154911
c
moDCs
E-MTAB-135
E-MTAB-751
623
27
29
57
340
4
1801
GSE77969
d
Intersection Size
167
65
42
29
14
12
2
moDCs
PBMCs
WBCs
Set Size
e
id
dendrogram_cut
GSE42606
GSE65088
GSE114180
GSE154911
GSE77969
E-MTAB-135
E-MTAB-751
PBMCs
WBCs
WBCs
PBMCs
moDCs
moDCs
moDCs
macrophage activation
interleukin-6 production
myeloid cell differentiation
CD4-positive, alpha-beta T cell activation
myeloid leukocyte differentiation
interleukin-1 beta production
regulation of T-helper cell differentiation
T cell differentiation
positive regulation of interleukin-2 production
regulation of cell-cell adhesion
ERK1 and ERK2 cascade
positive regulation of MAP kinase activity
positive regulation of receptor signaling pathway via JAK-STAT
positive regulation of receptor signaling pathway via STAT
positive regulation of tyrosine phosphorylation of STAT protein
myeloid leukocyte migration
response to tumor necrosis factor
positive regulation of NF-kappaB transcription factor activity
neutrophil migration
positive regulation of inflammatory response
positive regulation of T-helper cell differentiation
response to interleukin-1
JNK cascade
stress-activated MAPK cascade
I-kappaB kinase/NF-kappaB signaling
cellular response to interferon-gamma
negative regulation of viral life cycle
response to interferon-gamma
response to virus
Number of DEGs
2.00
6.00
10.00
-log10 adj. pvalue
0
10
20
f
id
WBCs
PBMCs
WBCs
WBCs
moDCs
PBMCs
moDCs
GSE65088
GSE42606
GSE77969
GSE114180
E-MTAB-135
GSE154911
E-MTAB-751
Toll Like Receptor 4 (TLR4) Cascade
MyD88:MAL(TIRAP) cascade initiated on plasma membrane
MyD88-independent TLR4 cascade
Toll Like Receptor 3 (TLR3) Cascade
Toll Like Receptor 9 (TLR9) Cascade
Toll Like Receptor 7/8 (TLR7/8) Cascade
Toll Like Receptor 10 (TLR10) Cascade
Toll Like Receptor 5 (TLR5) Cascade
Interleukin-17 signaling
MAP kinase activation
Toll Like Receptor TLR1:TLR2 Cascade
Toll Like Receptor TLR6:TLR2 Cascade
Toll Like Receptor 2 (TLR2) Cascade
Toll-like Receptor Cascades
Interleukin-1 family signaling
TAK1 activates NFkB by phosphorylation and activation of IKKs complex
NOD1/2 Signaling Pathway
NLR signaling pathways
Signaling by Interleukins
Interleukin-1 signaling
TRIF(TICAM1)-mediated TLR4 signaling
TRAF6 mediated induction of NFkB/MAPK upon TLR7/8 or 9 activation
MyD88 dependent cascade initiated on endosome
MyD88 cascade initiated on plasma membrane
Interleukin-6 family signaling
Interleukin-4 and Interleukin-13 signaling
Chemokine receptors bind chemokines
Interleukin-10 signaling
Interferon alpha/beta signaling
Interferon Signaling
Number of DEGs
2.00
8.50
15.00
-log10 adj. pvalue
0
5
10
g
Node color: Go biological process
Cell Aggregation
Cellular Component Organization of Biogenesis
Developmental Process
Immune System Process
Locomotion
Metabolic Process
Rhythmic Process
Signaling
Single-Organism Process
Growth
Uncategorized
C-type lectin receptors (CLRs)
CD209 (DC-SIGN) signaling
CLEC7A (Dectin-1) signaling
Dectin-1 mediated noncanonical NF-kB signaling
Inflammasomes
Interferon Signaling
Interferon alpha/beta signaling
Interferon gamma signaling
Interleukin-1 family signaling
Interleukin-10 signaling
Interleukin-12 family signaling
Interleukin-17 signaling
Interleukin-4 and Interleukin-13 signaling
Interleukin-6 family signaling
MAPK family signaling cascades
MyD88:MAL(TIRAP) cascade initiated on plasma membrane
NOD1/2 Signaling Pathway
Neutrophil degranulation
TAK1 activates NFkB by phosphorylation and activation of IKKs complex
TCR signaling
Toll Like Receptor 4 (TLR4) Cascade
Toll-like Receptor Cascades

Fig. 4. *C. albicans* activate common TLR and IFN signaling pathways across different layers of immunity. a-c, Venn diagrams displaying the number of DEGs present in each dataset grouped by cell type and their intersections: datasets of WBCs (a), PBMCs (b), and moDCs (c). **d,** The intersection plot highlights the number of common DEGs across different cell groups. **e,** Hierarchical clustering exhibiting the pathways enriching common biological processes across the studies (**Suppl. Table 9**). **f,** Further analysis of TLR- and IFN-associated pathways. In both heatmaps the size of circles corresponds to adjusted p-value transformed into -Log10 and color intensity indicates the number of genes in each biological process and pathway across the studies, respectively. **g,** Network demonstrating the interactions between TLR- and IFN-associated DEGs/signaling pathways with other molecules and signaling cascades classically associated with the antifungal immune responses. Enrichment analysis was performed using Reactome. Circular nodes represent pathways and their size denote the number of genes enriching the pathways. Colored squares represent the cellular location of genes. The interaction network was build using the NAViGaTOR software. *DEGs, Differentially Expressed Genes; moDCs, Monocyte-Derived Dendritic Cells; IFN, Interferon; PBMCs, Peripheral Blood Mononuclear Cells; TLR, Toll-like Receptor; WBCs, White Blood Cells.*

Figure 5

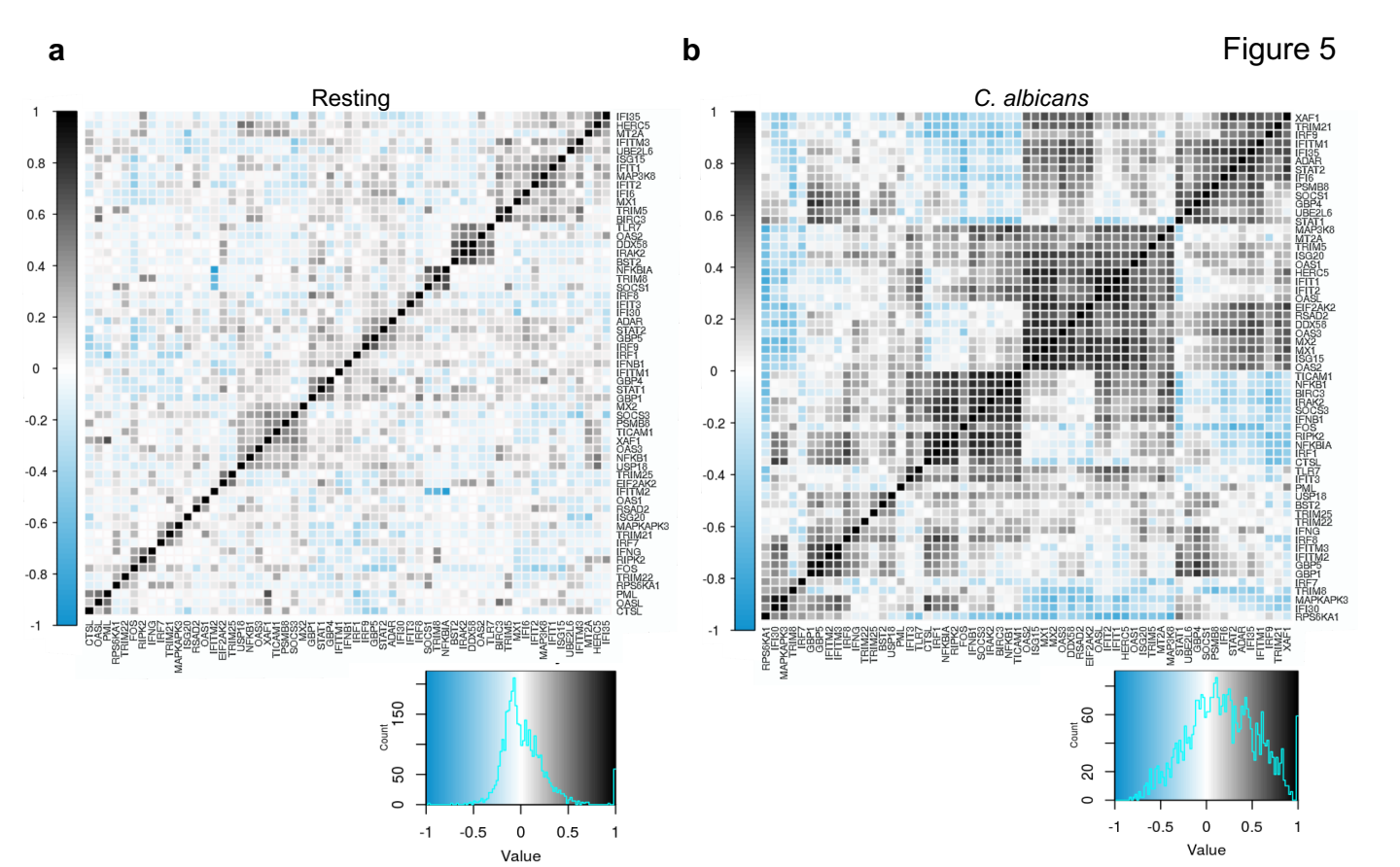
a
Resting
b
C. albicans
Count
Value

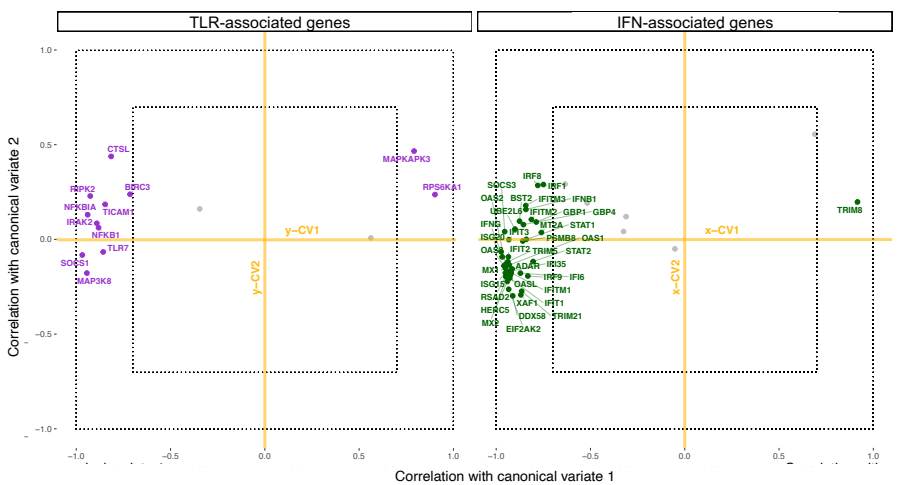
c
TLR-associated genes
IFN-associated genes
Correlation with canonical variate 2
Correlation with canonical variate 1
y–CV1
y–CV2
x–CV1
x–CV2

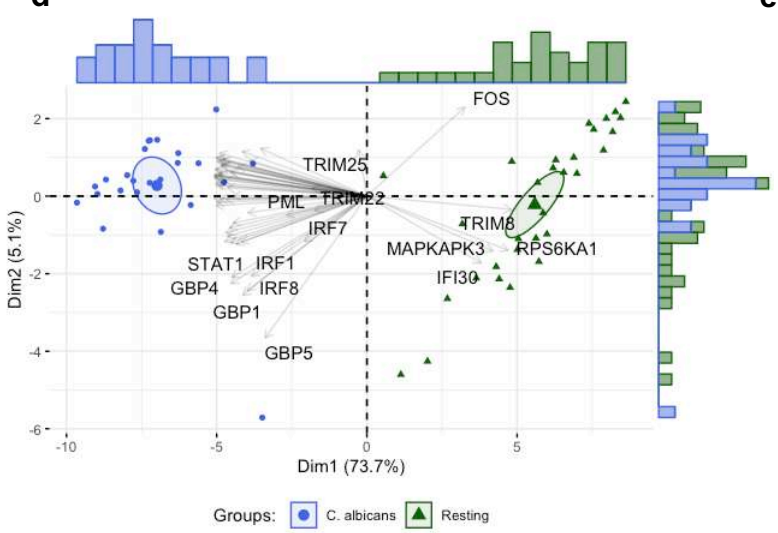
d
FOS
TRIM25
PML
TRIM22
IRF7
TRIM8
MAPKAPK3
RPS6KA1
IFI30
STAT1
IRF1
GBP4
IRF8
GBP1
GBP5
Dim2 (5.1%)
Dim1 (73.7%)
Groups:
C. albicans
Resting

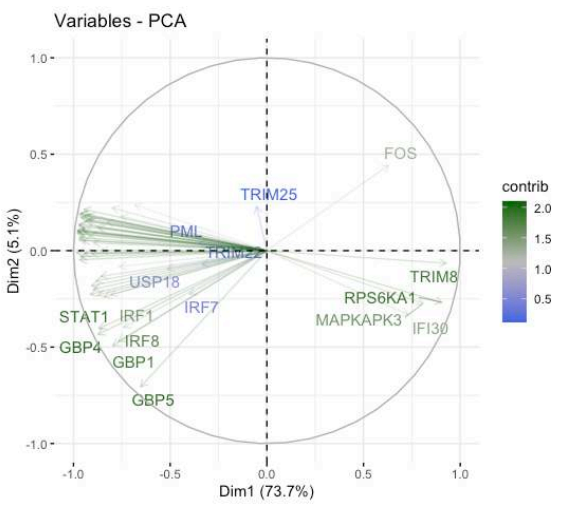
e
Variables - PCA
FOS
TRIM25
PML
TRIM22
USP18
IRF7
TRIM8
RPS6KA1
MAPKAPK3
IFI30
STAT1
IRF1
GBP4
IRF8
GBP1
GBP5
contrib
Dim2 (5.1%)
Dim1 (73.7%)

Fig. 5. Relationship between molecules associated with TLR and IFN signaling cascades. a,b, Correloplot of DEGs associated with TLR and IFN signaling cascades in PBMCs (GSE42606) in the **a,** absence or **b,** presence of *C. albicans.* Histograms of Pearson's correlation coefficient, containing negative and positive correlation from 1 to -1, respectively. **c,** Estimated correlations of TLR - and IFN -associated DEGs versus their corresponding first 2 canonical variates (x-CV1 and x-CV2, for IFN- associated genes; y-CV1 and y-CV2 for TLR-associated genes). Grey colored variables (with names omitted) are those with correlation coefficient ≤0.7 in its two corresponding canonical variates. Inner dotted lines limit the canonical correlation coefficient between -0.7 and 0.7, while outer dotted lines between -1 and 1**. d, e,** PCA was used for stratification analysis of resting and *C. albicans* infected PBMCs based on TLR- and IFN-associated DEGs. **d,** Of note, individuals with similar expression values for these DEGs are grouped together; **e,** Variables with positive correlation are pointing to same side of the plot, contrasting with negative correlated variables, which point to opposite sides. *DEGs, Differentially Expressed Genes; IFN, Interferon; PBMCs, Peripheral Blood Mononuclear Cells; TLR, Toll-like Receptor.*

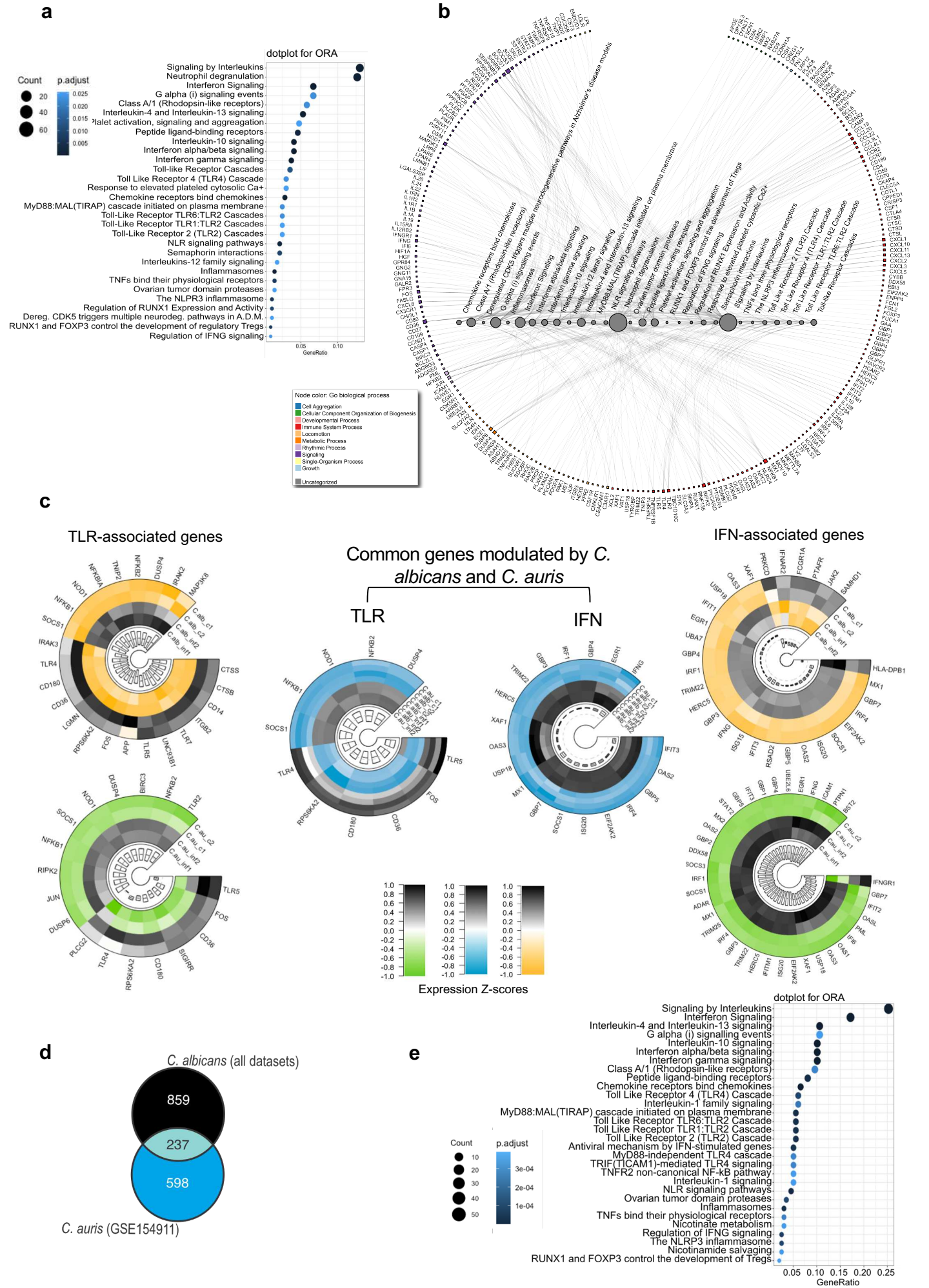
a
dotplot for ORA
Count
p.adjust
Signaling by Interleukins
Neutrophil degranulation
Interferon Signaling
G alpha (i) signaling events
Class A/1 (Rhodopsin-like receptors)
Interleukin-4 and Interleukin-13 signaling
Platelet activation, signaling and aggregation
Peptide ligand-binding receptors
Interleukin-10 signaling
Interferon alpha/beta signaling
Interferon gamma signaling
Toll-like Receptor Cascades
Toll Like Receptor 4 (TLR4) Cascade
Response to elevated plateled cytosolic Ca+
Chemokine receptors bind chemokines
MyD88:MAL(TIRAP) cascade initiated on plasma membrane
Toll-Like Receptor TLR6:TLR2 Cascades
Toll-Like Receptor TLR1:TLR2 Cascades
Toll-Like Receptor 2 (TLR2) Cascades
NLR signaling pathways
Semaphorin interactions
Interleukins-12 family signaling
Inflammasomes
TNFs bind their physiological receptors
Ovarian tumor domain proteases
The NLPR3 inflammasome
Regulation of RUNX1 Expression and Activity
Dereg. CDK5 triggers multiple neurodeg. pathways in A.D.M.
RUNX1 and FOXP3 control the development of regulatory Tregs
Regulation of IFNG signaling
GeneRatio
b
Node color: Go biological process
Cell Aggregation
Cellular Component Organization of Biogenesis
Developmental Process
Immune System Process
Locomotion
Metabolic Process
Rhythmic Process
Signaling
Single-Organism Process
Growth
Uncategorized
c
TLR-associated genes
Common genes modulated by C. albicans and C. auris
TLR
IFN
IFN-associated genes
C.alb_c1
C.alb_c2
C.alb_inf1
C.alb_inf2
C.au_c1
C.au_c2
C.au_inf1
C.au_inf2
Expression Z-scores
d
C. albicans (all datasets)
859
237
598
C. auris (GSE154911)
e
dotplot for ORA
Count
p.adjust
Signaling by Interleukins
Interferon Signaling
Interleukin-4 and Interleukin-13 signaling
G alpha (i) signalling events
Interleukin-10 signaling
Interferon alpha/beta signaling
Interferon gamma signaling
Class A/1 (Rhodopsin-like receptors)
Peptide ligand-binding receptors
Chemokine receptors bind chemokines
Toll Like Receptor 4 (TLR4) Cascade
Interleukin-1 family signaling
MyD88:MAL(TIRAP) cascade initiated on plasma membrane
Toll Like Receptor TLR6:TLR2 Cascade
Toll Like Receptor TLR1:TLR2 Cascade
Toll Like Receptor 2 (TLR2) Cascade
Antiviral mechanism by IFN-stimulated genes
MyD88-independent TLR4 cascade
TRIF(TICAM1)-mediated TLR4 signaling
TNFR2 non-canonical NF-kB pathway
Interleukin-1 signaling
NLR signaling pathways
Ovarian tumor domain proteases
Inflammasomes
TNFs bind their physiological receptors
Nicotinate metabolism
Regulation of IFNG signaling
The NLRP3 inflammasome
Nicotinamide salvaging
RUNX1 and FOXP3 control the development of Tregs
GeneRatio

Fig. 6. Induction of the interplay between TLR and IFN signaling pathways by the multidrug-resistant *C. auris*. a, Dot plot showing the 30 most enriched signaling pathways obtained by ORA of DEGs using ClusterProfiler. Y-axis contains enriched pathways while the size of circles represents the number of genes (count) enriching each category and color (from blue to black) indicating how significantly enriched (when p-value <0.05) is the pathway. **b,** Network demonstrating interactions between pathways and their associated genes revealed by ORA. Circular nodes represent pathways, circle size is associated with the number of genes enriching each pathway, while colored squares represent the cell location of genes. The interaction network was build using the NAViGaTOR software. **c,** Circular heatmaps of RNAseq expression z-scores computed for log2 transformed DEGs (p-value adj < 0.05, fold change > 1 and < -1) compares the expression of TLR- (left panels) and IFN- (right panels) signaling pathways induced by *C. albicans* (green/grey heatmaps) or *C. auris* (yellow/grey heatmaps) all from GSE154911. Small circular heatmaps (blue/grey) demonstrate common DEGs modulated by *C. abicans* and *C auris*. **d,** Venn diagram showing the transcriptional overlap (an intersection containing 237 shared DEGs) induced by *C. auris* and *C. albicans* (those 1096 genes found across all studies: **Suppl. Table 10)**. **e,** Dotplot of enriched pathways by the 237 shared DEGs. *DEGs, Differentially Expressed Genes; IFN, Interferon; ORA, Over representation analysis; TLR, Toll-like Receptor.*

Figure 7

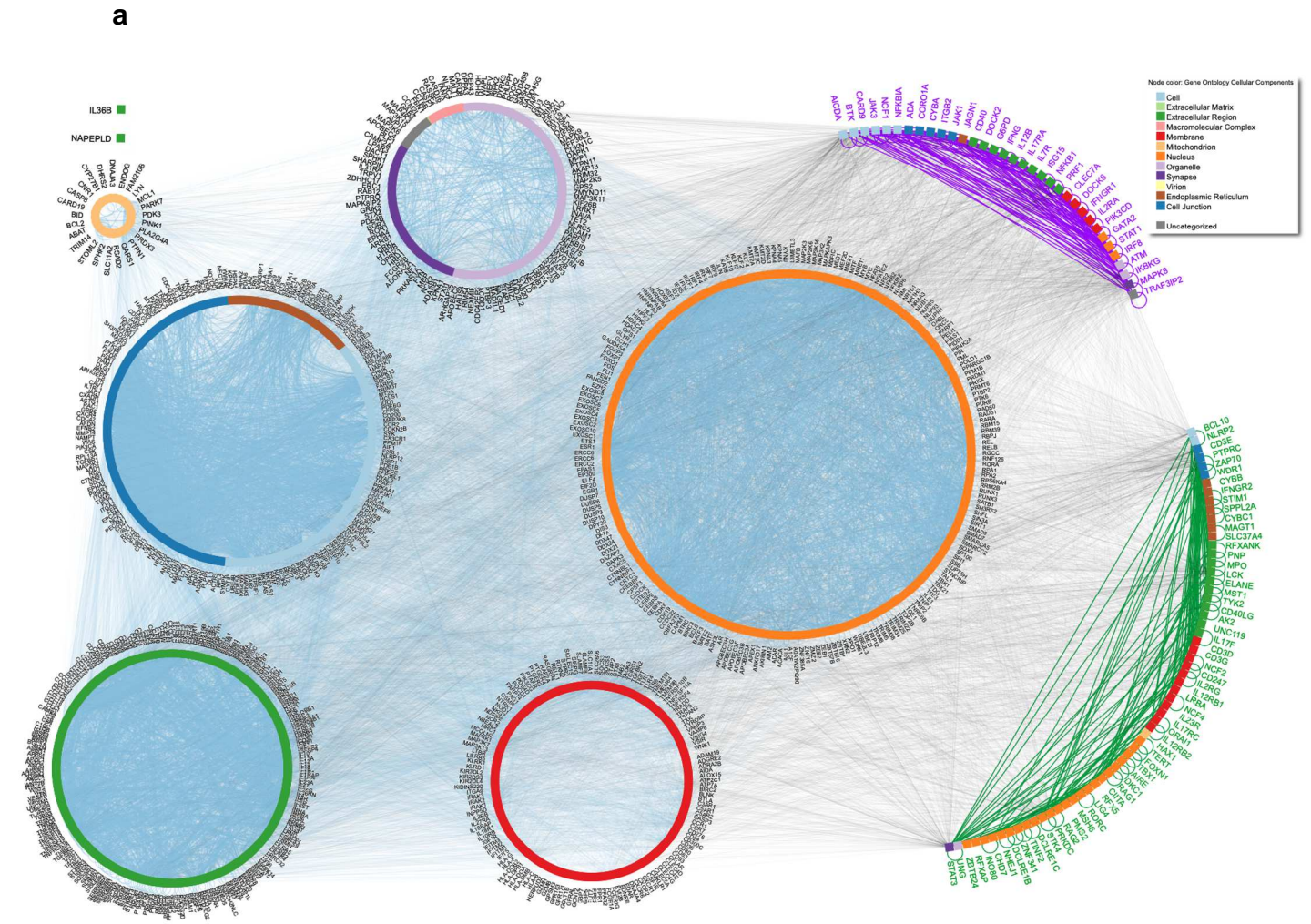
a
IL36B
NAPEPLD
Node color: Gene Ontology Cellular Components
Cell
Extracellular Matrix
Extracellular Region
Macromolecular Complex
Membrane
Mitochondrion
Nucleus
Organelle
Synapse
Virion
Endoplasmic Reticulum
Cell Junction
Uncategorized

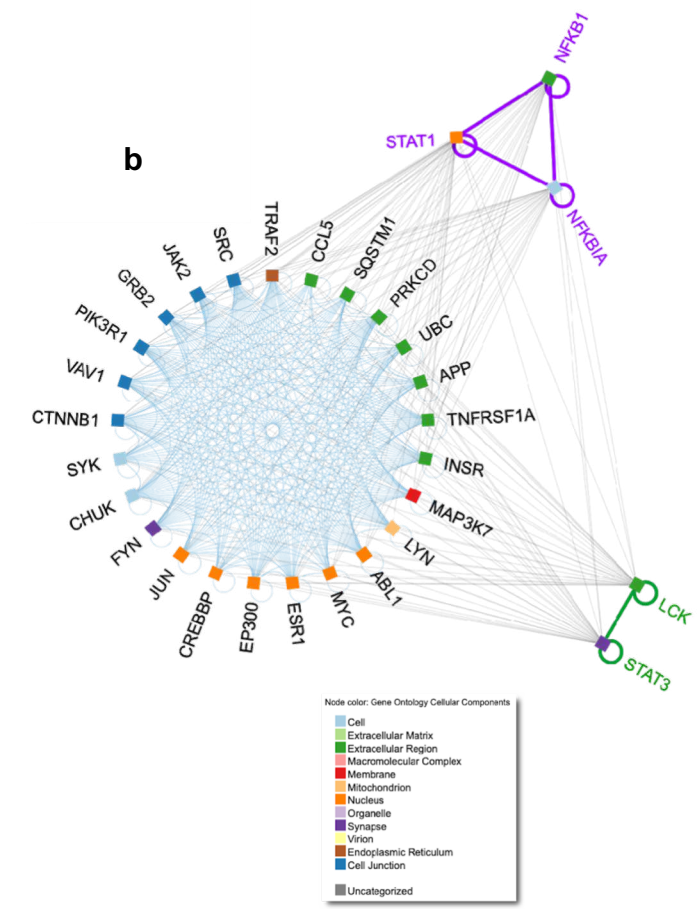
b
NFKB1
STAT1
NFKBIA
TRAF2
SRC
JAK2
GRB2
PIK3R1
VAV1
CTNNB1
SYK
CHUK
FYN
JUN
CREBBP
EP300
ESR1
MYC
ABL1
LYN
MAP3K7
INSR
TNFRSF1A
APP
UBC
PRKCD
SQSTM1
CCL5
LCK
STAT3
Node color: Gene Ontology Cellular Components
Cell
Extracellular Matrix
Extracellular Region
Macromolecular Complex
Membrane
Mitochondrion
Nucleus
Organelle
Synapse
Virion
Endoplasmic Reticulum
Cell Junction
Uncategorized

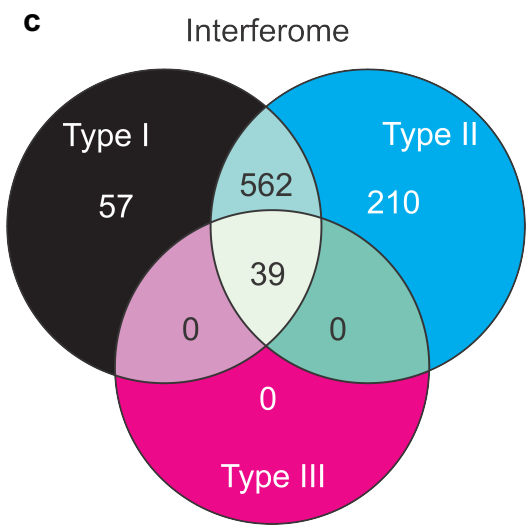
c
Interferome
Type I
57
562
Type II
210
39
0
0
0
Type III

Fig. 7. The interactome of DEGs enriching signaling pathways involved in the anti-candida immune response and its association with inborn errors of immunity. a, Relationships (edges) among the 1096 DEGs (nodes) found across all studies (**Suppl. Table 10**). Subnetworks (semicircles) represent genes associated with IEI causing increased susceptibility to candidiasis, being 34 purple nodes genes shared with the group of 1096 DEGs, while 66 green nodes represent those not found in the Candida datasets. Colored squares and circles represent the cell location of genes. The interaction network was build using the NAViGaTOR software. **b,** Network of hubs present in **a**. **c,** Venn diagram of interferon types associated with the group of 1096 DEGs. Interferome analysis revealed 868 IFN-regulated genes modulated either by IFN type I, II, and III, as in the Venn Diagram. *DEGs, Differentially Expressed Genes; IFN, Interferon; IEI, Inborn Errors of Immunity; TLR, Toll-like Receptor.*

Figure 8

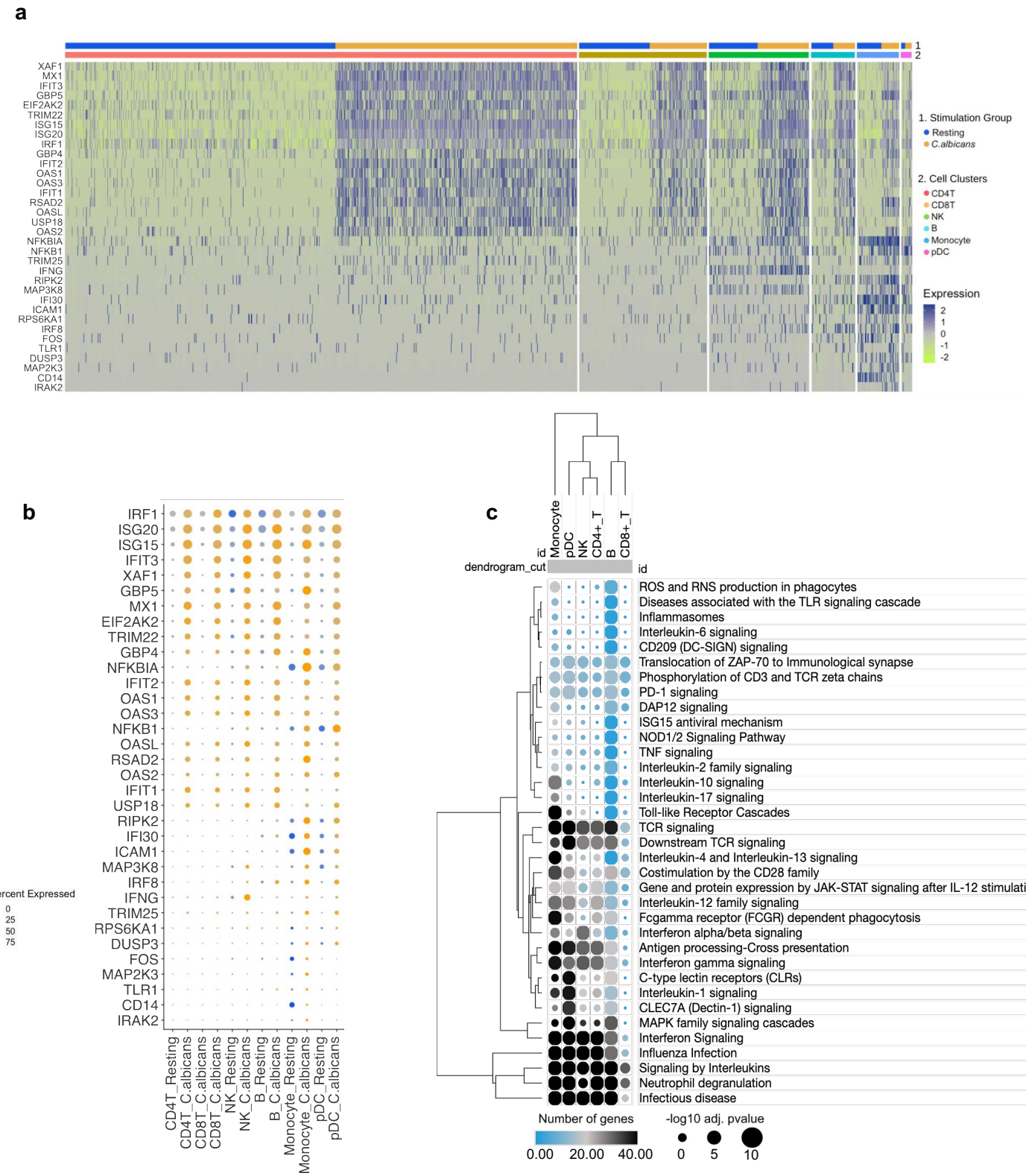
a
XAF1
MX1
IFIT3
GBP5
EIF2AK2
TRIM22
ISG15
ISG20
IRF1
GBP4
IFIT2
OAS1
OAS3
IFIT1
RSAD2
OASL
USP18
OAS2
NFKBIA
NFKB1
TRIM25
IFNG
RIPK2
MAP3K8
IFI30
ICAM1
RPS6KA1
IRF8
FOS
TLR1
DUSP3
MAP2K3
CD14
IRAK2
1
2
1. Stimulation Group
Resting
C.albicans
2. Cell Clusters
CD4T
CD8T
NK
B
Monocyte
pDC
Expression
2
1
0
-1
-2
b
IRF1
ISG20
ISG15
IFIT3
XAF1
GBP5
MX1
EIF2AK2
TRIM22
GBP4
NFKBIA
IFIT2
OAS1
OAS3
NFKB1
OASL
RSAD2
OAS2
IFIT1
USP18
RIPK2
IFI30
ICAM1
MAP3K8
IRF8
IFNG
TRIM25
RPS6KA1
DUSP3
FOS
MAP2K3
TLR1
CD14
IRAK2
CD4T_Resting
CD4T_C.albicans
CD8T_C.albicans
CD8T_C.albicans
NK_Resting
NK_C.albicans
B_Resting
B_C.albicans
Monocyte_Resting
Monocyte_C.albicans
pDC_Resting
pDC_C.albicans
Percent Expressed
0
25
50
75
c
id
Monocyte
pDC
NK
CD4+_T
B
CD8+_T
dendrogram_cut
id
ROS and RNS production in phagocytes
Diseases associated with the TLR signaling cascade
Inflammasomes
Interleukin-6 signaling
CD209 (DC-SIGN) signaling
Translocation of ZAP-70 to Immunological synapse
Phosphorylation of CD3 and TCR zeta chains
PD-1 signaling
DAP12 signaling
ISG15 antiviral mechanism
NOD1/2 Signaling Pathway
TNF signaling
Interleukin-2 family signaling
Interleukin-10 signaling
Interleukin-17 signaling
Toll-like Receptor Cascades
TCR signaling
Downstream TCR signaling
Interleukin-4 and Interleukin-13 signaling
Costimulation by the CD28 family
Gene and protein expression by JAK-STAT signaling after IL-12 stimulation
Interleukin-12 family signaling
Fcgamma receptor (FCGR) dependent phagocytosis
Interferon alpha/beta signaling
Antigen processing-Cross presentation
Interferon gamma signaling
C-type lectin receptors (CLRs)
Interleukin-1 signaling
CLEC7A (Dectin-1) signaling
MAPK family signaling cascades
Interferon Signaling
Influenza Infection
Signaling by Interleukins
Neutrophil degranulation
Infectious disease
Number of genes
0.00
20.00
40.00
-log10 adj. pvalue
0
5
10

Fig. 8. Common TLR- and IFN-associated DEGs and signaling pathways across microarray, bulk, and single-cell RNA-seq datasets. a, Heatmap using expression value from scRNAseq of DEGs also present in microarray and bulk studies; cell condition and group are indicated by different colors. **b,** Hierarchical clustering of average expression comparing resting and *C. albicans*-activated cells. **c,** Hierarchical clustering showing common pathways selected from Fig. 1d, across the cell groups; the size of circles corresponds to adjusted p-value transformed into -Log10 and color intensity indicates the number of genes in each pathway across the cell groups, respectively. *DEGs, Differentially Expressed Genes; IFN, Interferon; TLR, Toll-like Receptor; scRNAseq, single-cell RNA sequencing.*

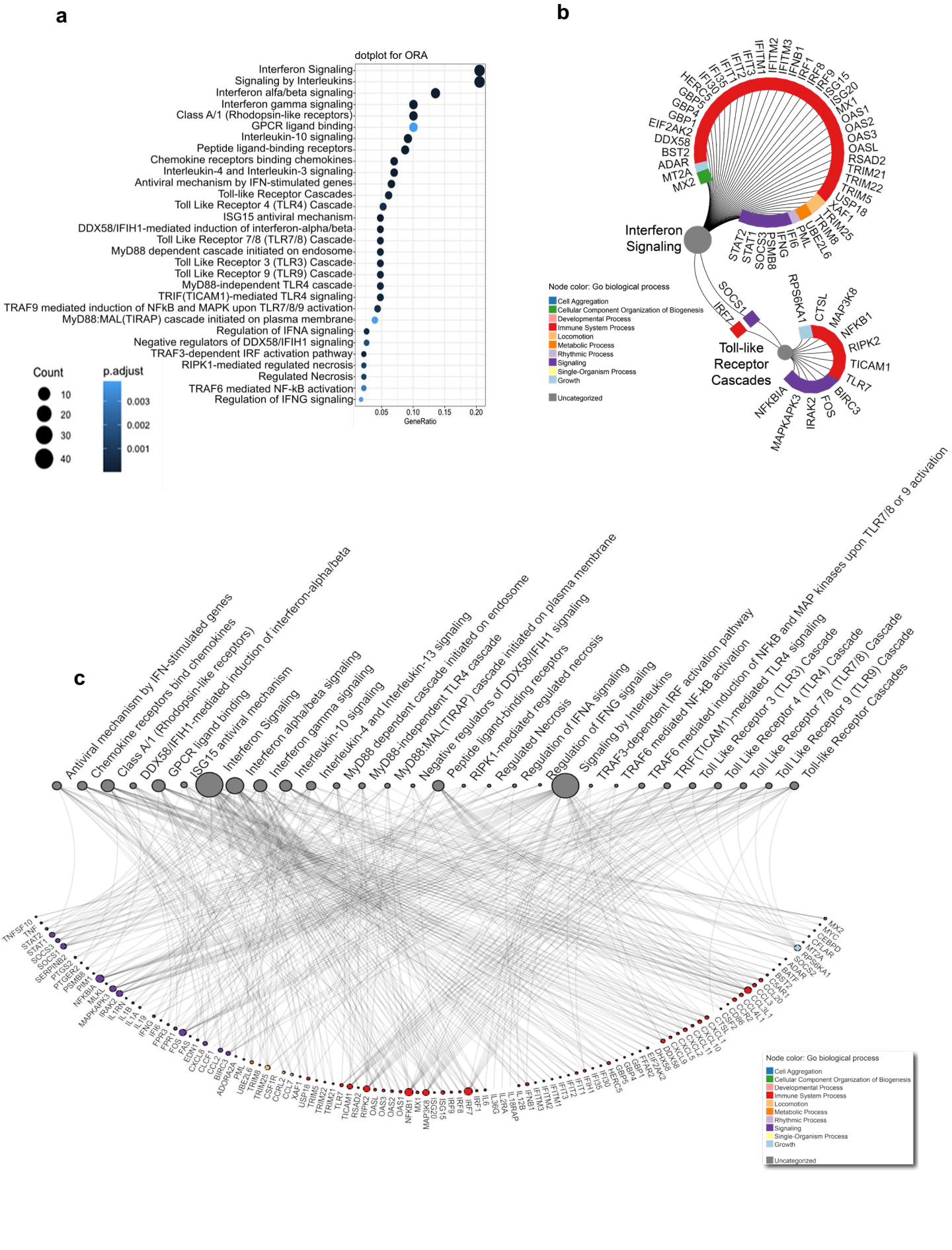
a
dotplot for ORA
Interferon Signaling
Signaling by Interleukins
Interferon alfa/beta signaling
Interferon gamma signaling
Class A/1 (Rhodopsin-like receptors)
GPCR ligand binding
Interleukin-10 signaling
Peptide ligand-binding receptors
Chemokine receptors binding chemokines
Interleukin-4 and Interleukin-3 signaling
Antiviral mechanism by IFN-stimulated genes
Toll-like Receptor Cascades
Toll Like Receptor 4 (TLR4) Cascade
ISG15 antiviral mechanism
DDX58/IFIH1-mediated induction of interferon-alpha/beta
Toll Like Receptor 7/8 (TLR7/8) Cascade
MyD88 dependent cascade initiated on endosome
Toll Like Receptor 3 (TLR3) Cascade
Toll Like Receptor 9 (TLR9) Cascade
MyD88-independent TLR4 cascade
TRIF(TICAM1)-mediated TLR4 signaling
TRAF9 mediated induction of NFkB and MAPK upon TLR7/8/9 activation
MyD88:MAL(TIRAP) cascade initiated on plasma membrane
Regulation of IFNA signaling
Negative regulators of DDX58/IFIH1 signaling
TRAF3-dependent IRF activation pathway
RIPK1-mediated regulated necrosis
Regulated Necrosis
TRAF6 mediated NF-kB activation
Regulation of IFNG signaling
0.05
0.10
0.15
0.20
GeneRatio
Count
10
20
30
40
p.adjust
0.003
0.002
0.001
b
Interferon Signaling
Toll-like Receptor Cascades
Node color: Go biological process
Cell Aggregation
Cellular Component Organization of Biogenesis
Developmental Process
Immune System Process
Locomotion
Metabolic Process
Rhythmic Process
Signaling
Single-Organism Process
Growth
Uncategorized
c
Antiviral mechanism by IFN-stimulated genes
Chemokine receptors bind chemokines
Class A/1 (Rhodopsin-like receptors)
DDX58/IFIH1-mediated induction of interferon-alpha/beta
GPCR ligand binding
ISG15 antiviral mechanism
Interferon Signaling
Interferon alpha/beta signaling
Interferon gamma signaling
Interleukin-10 signaling
Interleukin-4 and Interleukin-13 signaling
MyD88 dependent cascade initiated on endosome
MyD88-independent TLR4 cascade
MyD88:MAL(TIRAP) cascade initiated on plasma membrane
Negative regulators of DDX58/IFIH1 signaling
Peptide ligand-binding receptors
RIPK1-mediated regulated necrosis
Regulated Necrosis
Regulation of IFNA signaling
Regulation of IFNG signaling
Signaling by Interleukins
TRAF3-dependent IRF activation pathway
TRAF6 mediated NF-kB activation
TRAF6 mediated induction of NFkB and MAP kinases upon TLR7/8 or 9 activation
TRIF(TICAM1)-mediated TLR4 signaling
Toll Like Receptor 3 (TLR3) Cascade
Toll Like Receptor 4 (TLR4) Cascade
Toll Like Receptor 7/8 (TLR7/8) Cascade
Toll Like Receptor 9 (TLR9) Cascade
Toll-like Receptor Cascades
Node color: Go biological process
Cell Aggregation
Cellular Component Organization of Biogenesis
Developmental Process
Immune System Process
Locomotion
Metabolic Process
Rhythmic Process
Signaling
Single-Organism Process
Growth
Uncategorized

Suppl. Fig. 1. Functional clustering of DEGs associates TLR and IFN signaling pathways. a, Dot plot showing the 30 most enriched signaling pathways obtained by ORA of DEGs (dataset GSE42606) using ClusterProfiler. Y-axis contains enriched pathways while the size of circles represents the number of genes (count) enriching each category and color (from blue to black) indicates how significant (when p-value < 0.05) enriched is the pathway. **b,** Network of TLR- and IFN-associated genes enriching signaling pathways showed in the dot plot (a). The network includes genes upregulated and downregulated (**Suppl. Table 4**) when comparing resting with *C. albicans*-infected PBMCs. The size of circles represents the number (counts) of genes that enrich the pathway, and colored squares represent the cell location of genes. **c,** Network demonstrating interactions between pathways and their associated genes revealed by ORA. Circular nodes represent pathways and the circle size is associated with the number of genes that enrich each pathway, while colored squares represent the cell location of genes. The interaction network was build using the NAViGaTOR software. *DEGs, Differentially Expressed Genes; IFN, Interferon; ORA, Over-representation Analysis; TLR, Toll-like Receptor.*

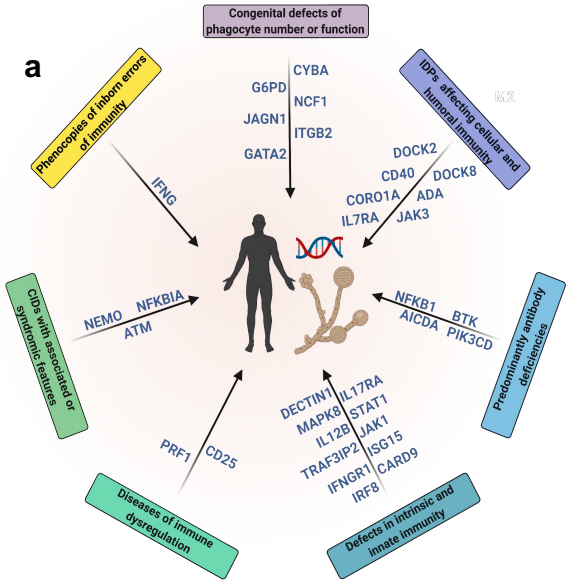
a
Congenital defects of phagocyte number or function
Phenocopies of inborn errors of immunity
IDPs affecting cellular and humoral immunity
CYBA
G6PD
NCF1
JAGN1
ITGB2
GATA2
IFNG
DOCK2
CD40
DOCK8
CORO1A
ADA
IL7RA
JAK3
CIDs with associated or syndromic features
NEMO
NFKBIA
ATM
Predominantly antibody deficiencies
NFKB1
BTK
AICDA
PIK3CD
Diseases of immune dysregulation
PRF1
CD25
Defects in intrinsic and innate immunity
DECTIN1
IL17RA
MAPK8
STAT1
IL12B
JAK1
TRAF3IP2
ISG15
IFNGR1
CARD9
IRF8

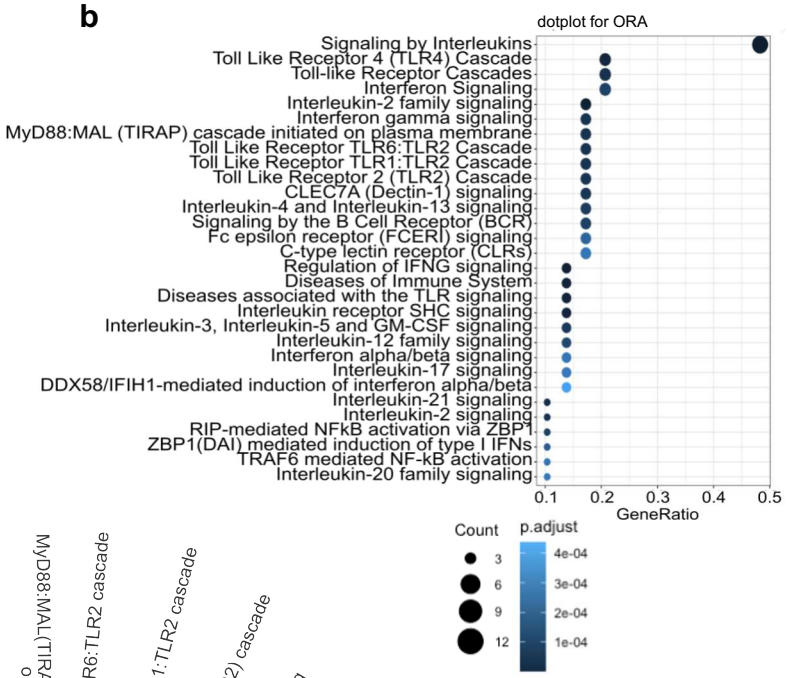
b
dotplot for ORA
Signaling by Interleukins
Toll Like Receptor 4 (TLR4) Cascade
Toll-like Receptor Cascades
Interferon Signaling
Interleukin-2 family signaling
Interferon gamma signaling
MyD88:MAL (TIRAP) cascade initiated on plasma membrane
Toll Like Receptor TLR6:TLR2 Cascade
Toll Like Receptor TLR1:TLR2 Cascade
Toll Like Receptor 2 (TLR2) Cascade
CLEC7A (Dectin-1) signaling
Interleukin-4 and Interleukin-13 signaling
Signaling by the B Cell Receptor (BCR)
Fc epsilon receptor (FCERI) signaling
C-type lectin receptor (CLRs)
Regulation of IFNG signaling
Diseases of Immune System
Diseases associated with the TLR signaling
Interleukin receptor SHC signaling
Interleukin-3, Interleukin-5 and GM-CSF signaling
Interleukin-12 family signaling
Interferon alpha/beta signaling
Interleukin-17 signaling
DDX58/IFIH1-mediated induction of interferon alpha/beta
Interleukin-21 signaling
Interleukin-2 signaling
RIP-mediated NFkB activation via ZBP1
ZBP1(DAI) mediated induction of type I IFNs
TRAF6 mediated NF-kB activation
Interleukin-20 family signaling
0.1
0.2
0.3
0.4
0.5
GeneRatio
Count
3
6
9
12
p.adjust
4e-04
3e-04
2e-04
1e-04

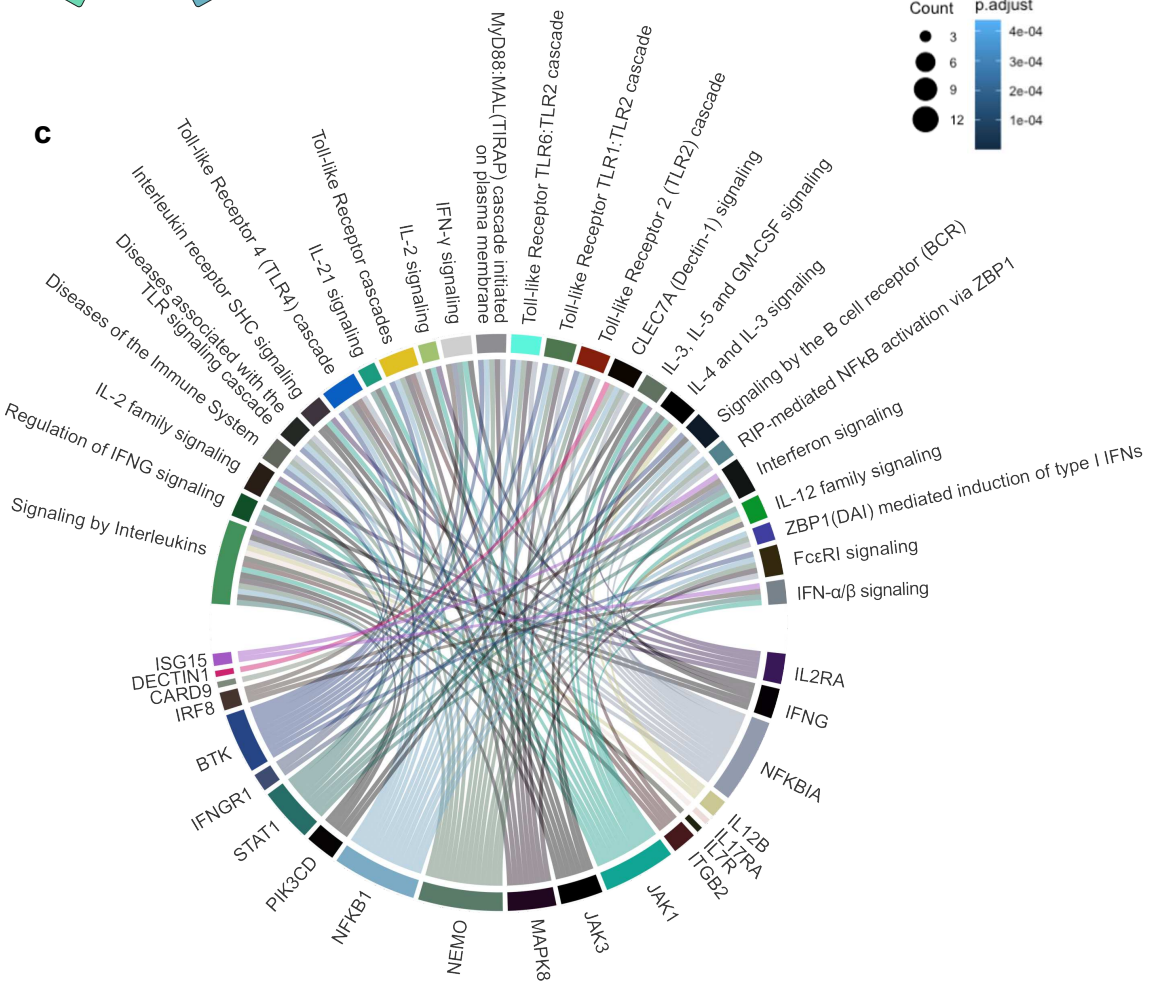
c
MyD88:MAL(TIRAP) cascade initiated on plasma membrane
Toll-like Receptor TLR6:TLR2 cascade
Toll-like Receptor TLR1:TLR2 cascade
Toll-like Receptor 2 (TLR2) cascade
CLEC7A (Dectin-1) signaling
IL-3, IL-5 and GM-CSF signaling
IL-4 and IL-3 signaling
Signaling by the B cell receptor (BCR)
RIP-mediated NFkB activation via ZBP1
Interferon signaling
IL-12 family signaling
ZBP1(DAI) mediated induction of type I IFNs
FcεRI signaling
IFN-α/β signaling
IL-2 signaling
IFN-γ signaling
Toll-like Receptor Cascades
IL-21 signaling
Toll-like Receptor 4 (TLR4) cascade
Interleukin receptor SHC signaling
Diseases associated with the TLR signaling cascade
Diseases of the Immune System
IL-2 family signaling
Regulation of IFNG signaling
Signaling by Interleukins
IL2RA
IFNG
NFKBIA
IL12B
IL17RA
ITGB2
JAK1
JAK3
MAPK8
NEMO
NFKB1
PIK3CD
STAT1
IFNGR1
BTK
IRF8
CARD9
DECTIN1
ISG15

Suppl. Fig. 2. Inborn errors of immunity confirm the interplay of TLR- and IFN-associated genes. a, Overview (created using BioRender.com) of genes associated with inborn errors of immunity that are also found among the DEGs across the 7 datasets of WBCs, PBMCs, and moDCs (**Suppl. Table 14**). **b,** Dot plot showing the 30 most enriched signaling pathways obtained by ORA of DEGs seen in (**a**). Y-axis contains enriched pathways while the size of circles represents the number of genes (count) enriching each category and color (from blue to black) indicates how significantly enriched (when p-value <0.05) is each pathway. **c,** GOPlot displaying genes causing inborn errors of immunity and enriched pathways. *DEGs, Differentially Expressed Genes; moDCs, Monocyte-Derived Dendritic Cells; IFN, Interferon; ORA, Over-representation Analysis; PBMCs, Peripheral Blood Mononuclear Cells; TLR, Toll-like Receptor; WBCs, White Blood Cells.*

Figures

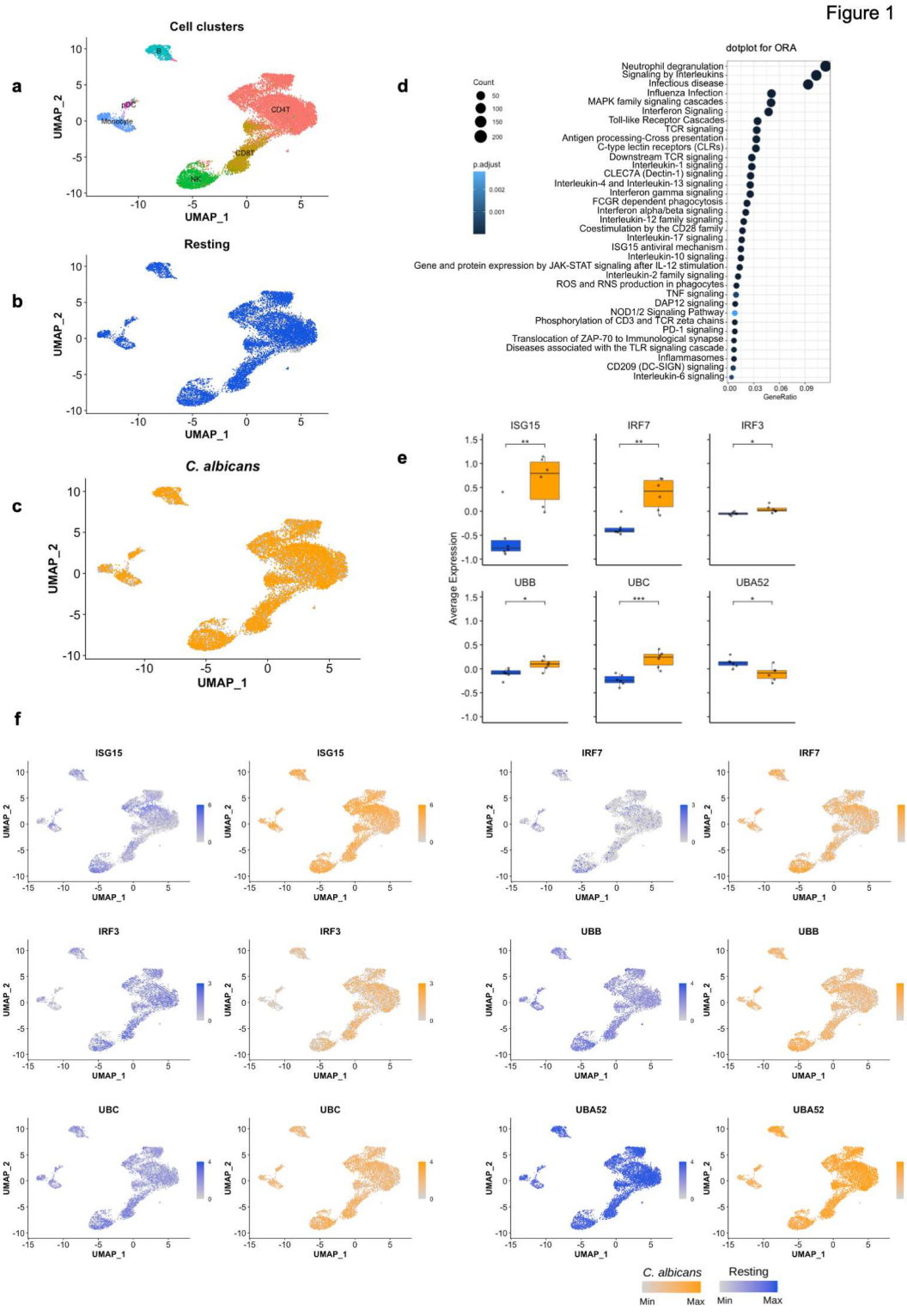

Figure 1

scRNAseq revealed common activation of TLR and IFN signaling pathways. a, UMAP visualization of scRNAseq profiles colored according to cell clusters. b, c, UMAP of resting and C. albicans-activated cells groups. d, Dot plot showing pathways associated with immune response to C. albicans, obtained by ORA

of DEGs. e, Boxplot and f, UMAP of DEGs associated with both TLR and IFN signaling pathways, additional DEGs associated with these two pathways are described in Suppl. Table 3. DEGs, Differentially Expressed Genes; IFN, Interferon; ORA, Over representation analysis; scRNAseq, single-cell RNA sequencing; TLR, Toll-like Receptor; UMAP, Uniform Manifold Approximation and Projection.

Figure 2

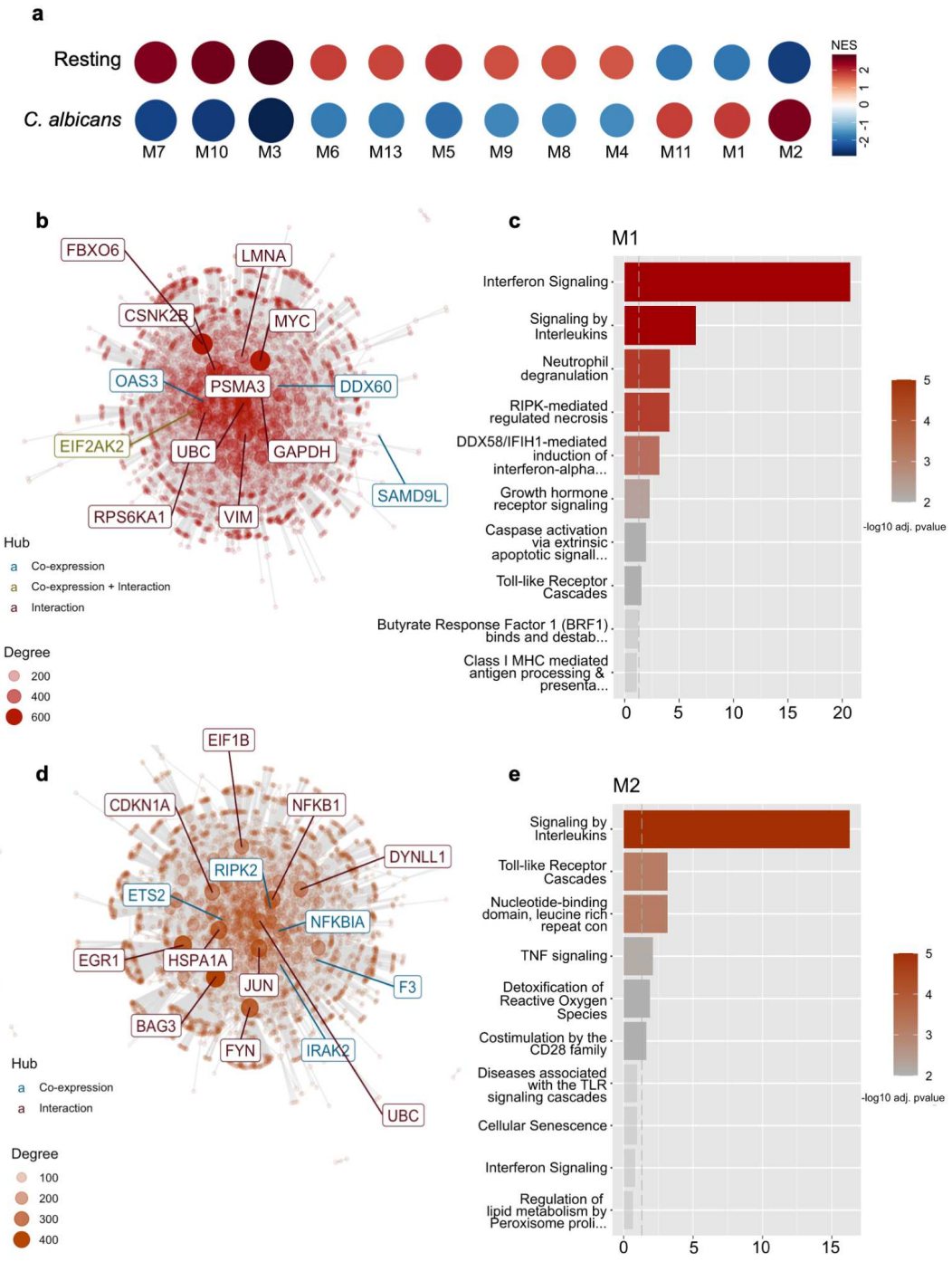

Figure 2

Modular gene co-expression analysis and the association of TLR and IFN signaling pathways. a, Co-expression modules significantly enriched (M1-M11, and M13) in PBMCs (resting n= 30; C. albicans infected n= 24; dataset GSE42606). b and d Network representation of M1 and M2 with hubs (most connected genes) colored based on coexpression (blue color), co-expressed and interactions (green color), or only interactions (dark-red color). c and e, Enrichment representation obtained by modular genes coexpression in M1 and M2 showing significantly (-Log10 transformed adjusted p-value) enriched signaling pathways. IFN, Interferon; TLR, Toll-like Receptor.

Figure 3

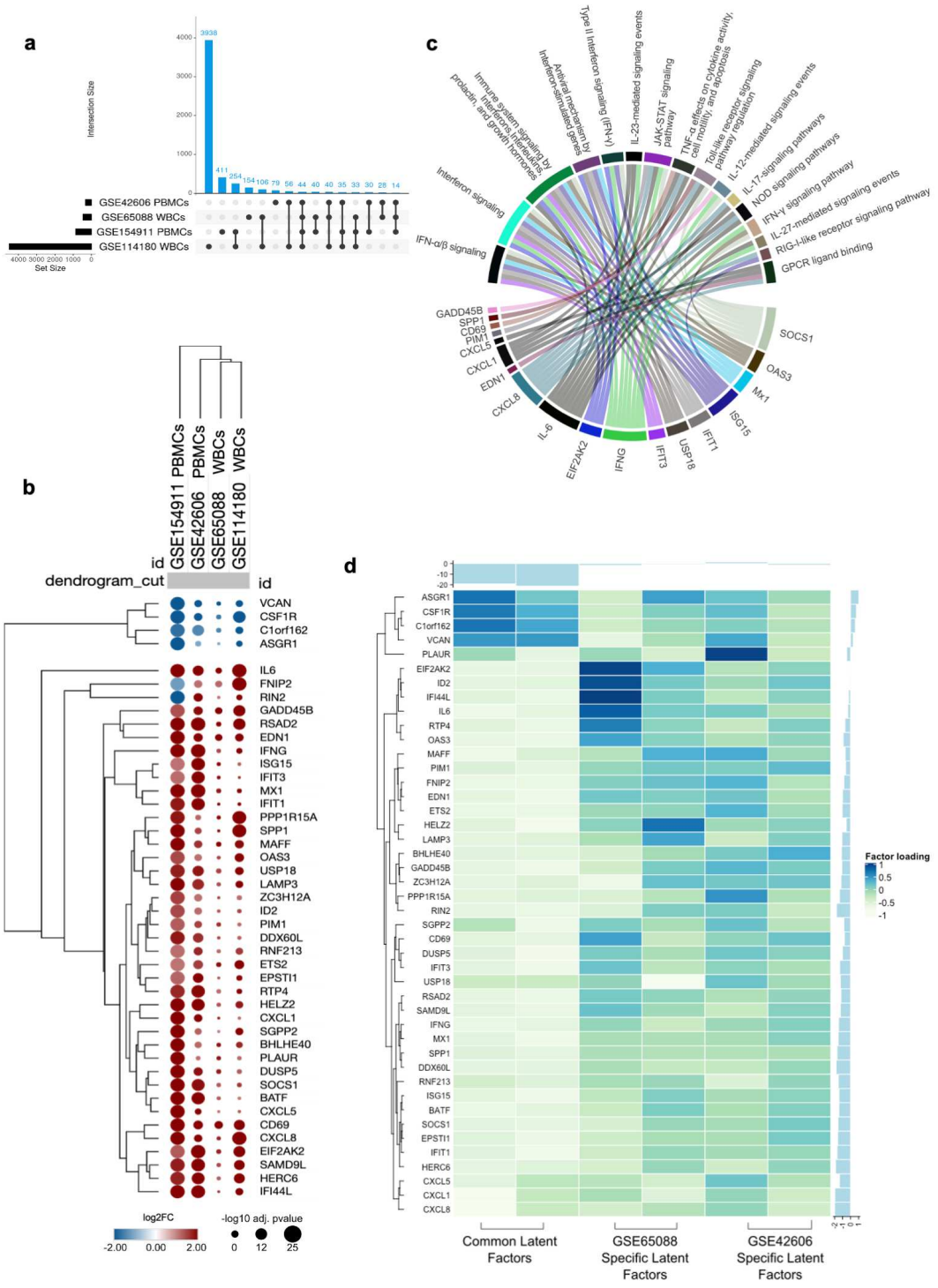

Figure 3

C. albicans activates common TLR- and IFN-associated genes in peripheral blood leukocytes. a, The upset plot displays the number (set size) of DEGs present in each dataset (y-axis: WBCs, GSE65088, and GSE114180; PBMCs: GSE42606 and GSE154911) and their intersections. Black bubbles, present in the rows, mark the dataset which refers to the amount present in the blue columns, with intersections between two or more groups being shown. b, Hierarchical clustering of the 44 common DEGs demonstrating gene expression patterns across the different studies. The size and color of circles correspond to -Log10 transformed adjusted p-value and Log2 fold change (Log2FC), respectively. Blue represents downregulated and red indicates up-regulated DEGs. The cut-off applied to identify the down-/upregulated genes was Log2FC < -1/> 1 and adjusted p-value < 0.05. Rows and columns were clustered based on cosine similarity between Log2FC values. c, GOplot of selected immunological pathways and associated gene. d, Heatmap of common and specific latent factors across the studies. Heatmaps contain genes presenting positive and negative loadings ranging from -1 to 1. DEGs, Differentially Expressed Genes; PBMCs, Peripheral Blood Mononuclear Cells; WBCs, White Blood Cells.

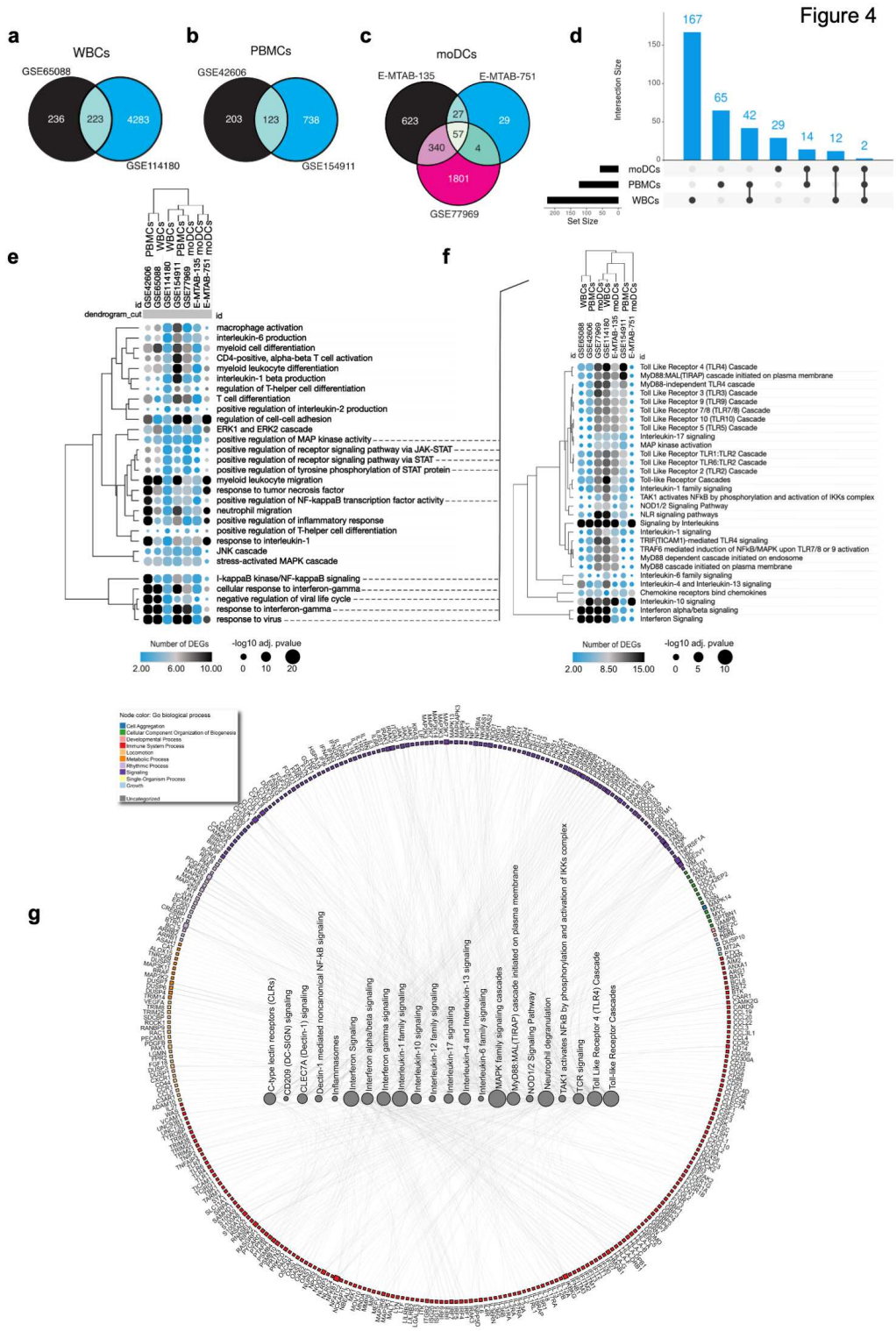

Figure 4

C. albicans activate common TLR and IFN signaling pathways across different layers of immunity. a-c, Venn diagrams displaying the number of DEGs present in each dataset grouped by cell type and their intersections: datasets of WBCs (a), PBMCs (b), and moDCs (c). d, The intersection plot highlights the number of common DEGs across different cell groups. e, Hierarchical clustering exhibiting the pathways enriching common biological processes across the studies (Suppl. Table 9). f, Further analysis of TLR-

and IFNassociated pathways. In both heatmaps the size of circles corresponds to adjusted p-value transformed into -Log10 and color intensity indicates the number of genes in each biological process and pathway across the studies, respectively. g, Network demonstrating the interactions between TLR- and IFN-associated DEGs/signaling pathways with other molecules and signaling cascades classically associated with the antifungal immune responses. Enrichment analysis was performed using Reactome. Circular nodes represent pathways and their size denote the number of genes enriching the pathways. Colored squares represent the cellular location of genes. The interaction network was build using the NAViGaTOR software. DEGs, Differentially Expressed Genes; moDCs, Monocyte-Derived Dendritic Cells; IFN, Interferon; PBMCs, Peripheral Blood Mononuclear Cells; TLR, Toll-like Receptor; WBCs, White Blood Cells.

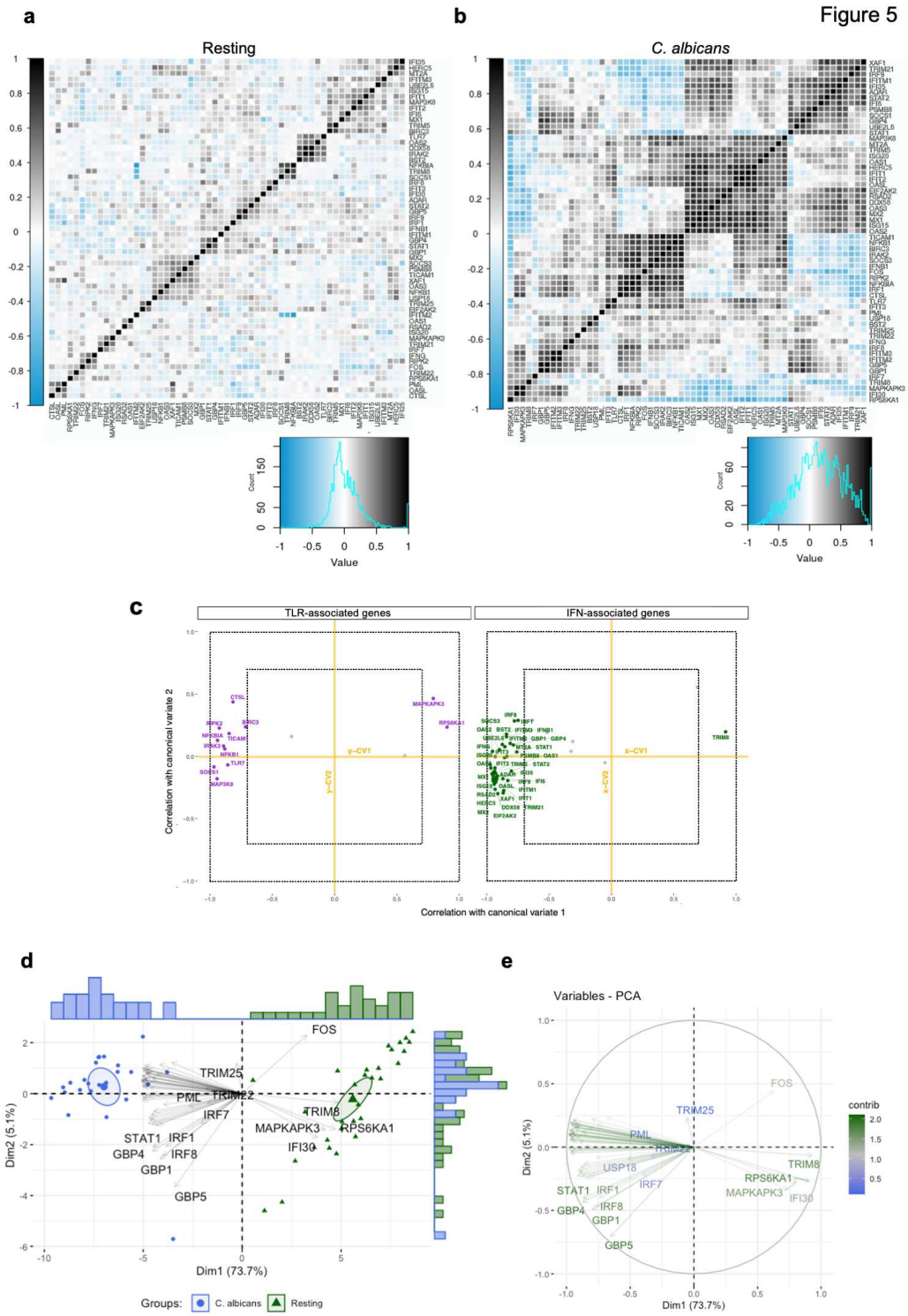

Figure 5

Relationship between molecules associated with TLR and IFN signaling cascades. a,b, Correloplot of DEGs associated with TLR and IFN signaling cascades in PBMCs (GSE42606) in the a, absence or b, presence of C. albicans. Histograms of Pearson's correlation coefficient, containing negative and positive correlation from 1 to -1, respectively. c, Estimated correlations of TLR - and IFN -associated DEGs versus their corresponding first 2 canonical variates (x-CV1 and x-CV2, for IFN- associated genes; y-CV1 and y-

CV2 for TLR-associated genes). Grey colored variables (with names omitted) are those with correlation coefficient ≤0.7 in its two corresponding canonical variates. Inner dotted lines limit the canonical correlation coefficient between -0.7 and 0.7, while outer dotted lines between -1 and 1. d, e, PCA was used for stratification analysis of resting and C. albicans infected PBMCs based on TLR- and IFN-associated DEGs. d, Of note, individuals with similar expression values for these DEGs are grouped together; e, Variables with positive correlation are pointing to same side of the plot, contrasting with negative correlated variables, which point to opposite sides. DEGs, Differentially Expressed Genes; IFN, Interferon; PBMCs, Peripheral Blood Mononuclear Cells; TLR, Toll-like Receptor

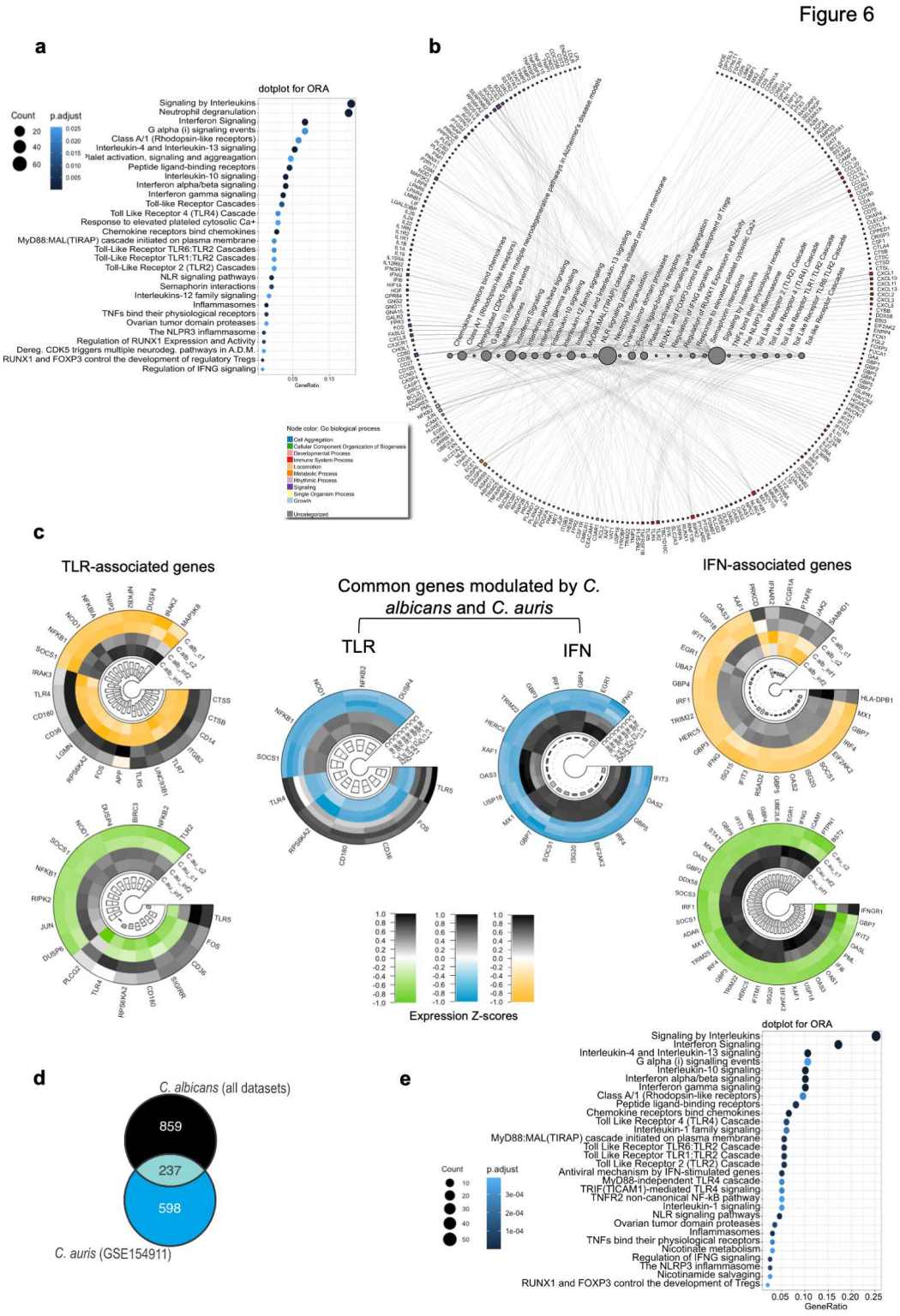

Figure 6

Induction of the interplay between TLR and IFN signaling pathways by the multidrug-resistant C. auris. a, Dot plot showing the 30 most enriched signaling pathways obtained by ORA of DEGs using ClusterProfiler. Y-axis contains enriched pathways while the size of circles represents the number of genes (count) enriching each category and color (from blue to black) indicating how significantly enriched (when p-value <0.05) is the pathway. b, Network demonstrating interactions between pathways

and their associated genes revealed by ORA. Circular nodes represent pathways, circle size is associated with the number of genes enriching each pathway, while colored squares represent the cell location of genes. The interaction network was build using the NAViGaTOR software. c, Circular heatmaps of RNAseq expression z-scores computed for log2 transformed DEGs (p-value adj < 0.05, fold change > 1 and < -1) compares the expression of TLR- (left panels) and IFN- (right panels) signaling pathways induced by C. albicans (green/grey heatmaps) or C. auris (yellow/grey heatmaps) all from GSE154911. Small circular heatmaps (blue/grey) demonstrate common DEGs modulated by C. abicans and C auris. d, Venn diagram showing the transcriptional overlap (an intersection containing 237 shared DEGs) induced by C. auris and C. albicans (those 1096 genes found across all studies: Suppl. Table 10). e, Dotplot of enriched pathways by the 237 shared DEGs. DEGs, Differentially Expressed Genes; IFN, Interferon; ORA, Over representation analysis; TLR, Toll-like Receptor.

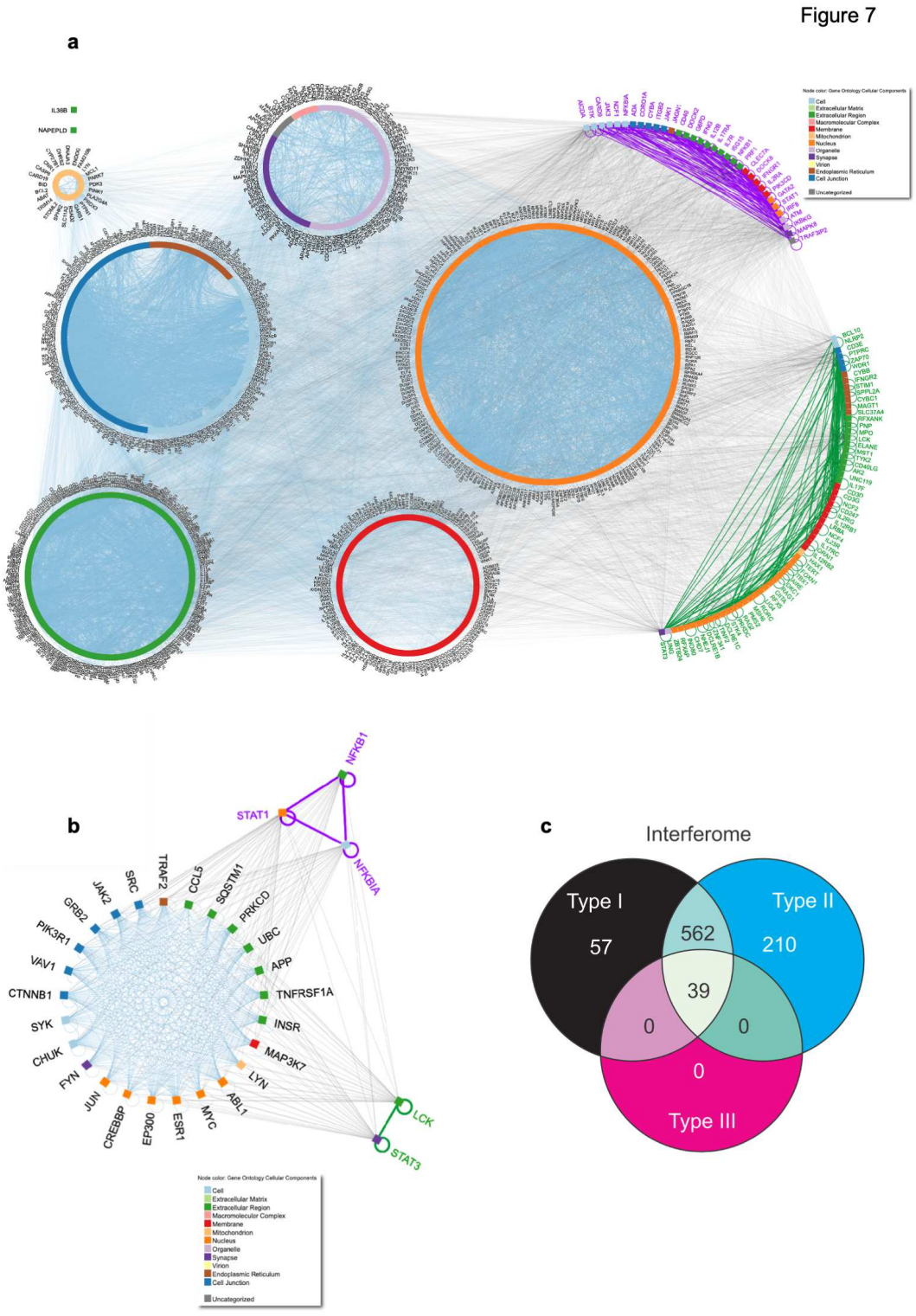

Figure 7

The interactome of DEGs enriching signaling pathways involved in the anticandida immune response and its association with inborn errors of immunity. a, Relationships (edges) among the 1096 DEGs (nodes) found across all studies (Suppl. Table 10). Subnetworks (semicircles) represent genes associated with IEI causing increased susceptibility to candidiasis, being 34 purple nodes genes shared with the group of 1096 DEGs, while 66 green nodes represent those not found in the Candida datasets. Colored

squares and circles represent the cell location of genes. The interaction network was build using the NAViGaTOR software. b, Network of hubs present in a. c, Venn diagram of interferon types associated with the group of 1096 DEGs. Interferome analysis revealed 868 IFN-regulated genes modulated either by IFN type I, II, and III, as in the Venn Diagram. DEGs, Differentially Expressed Genes; IFN, Interferon; IEI, Inborn Errors of Immunity; TLR, Toll-like Receptor.

Figure 8

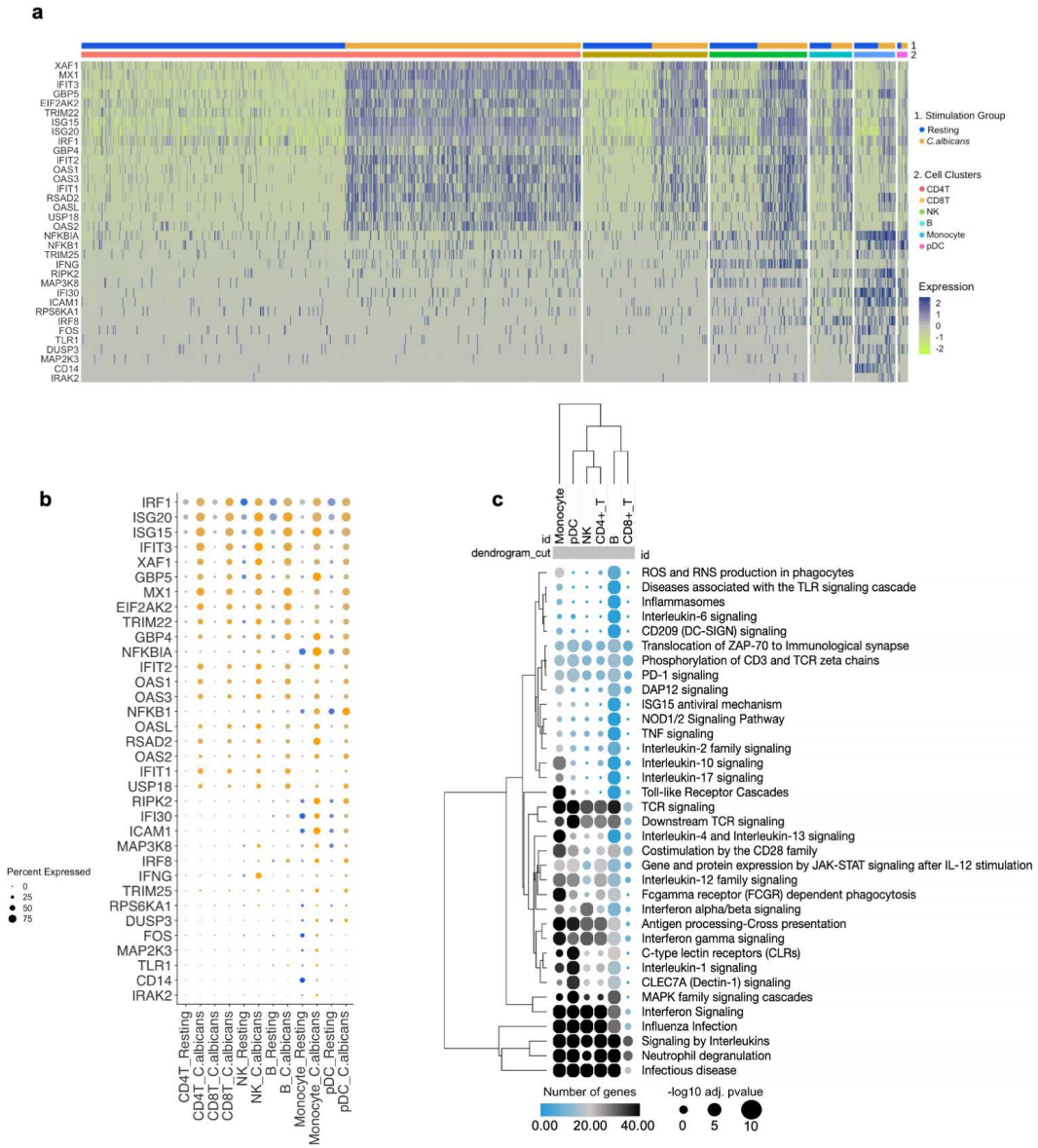

Figure 8

Common TLR- and IFN-associated DEGs and signaling pathways across microarray, bulk, and single-cell RNA-seq datasets. a, Heatmap using expression value from scRNAseq of DEGs also present in microarray and bulk studies; cell condition and group are indicated by different colors. b, Hierarchical clustering of average expression comparing resting and C. albicans-activated cells. c, Hierarchical clustering showing common pathways selected from Fig. 1d, across the cell groups; the size of circles corresponds to adjusted p-value transformed into -Log10 and color intensity indicates the number of genes in each pathway across the cell groups, respectively. DEGs, Differentially Expressed Genes; IFN, Interferon; TLR, Toll-like Receptor; scRNAseq, single-cell RNA sequencing.

Supplementary Files

This is a list of supplementary files associated with this preprint. Click to download.

- SupplementaryTablesS1S14.xlsx
- Graphicabstract.tiff
- Suppl.Figure1.tiff
- Suppl.Figure2.tiff